EFFECT OF REPEATED CYCLIC LATERAL LOADING ON LOAD BEARING SHEAR WALL PANELS

EFFECT OF REPEATED CYCLIC LATERAL LOADING ON LOAD BEARING SHEAR WALL PANELS

by

D.J. de LISLE, B.E. (HONS.)

A Thesis

Submitted to the School of Graduate Studies

in Partial Fulfilment of the Requirements

for the Degree

Master of Engineering

McMaster University

April 1971

MASTER OF ENGINEERING (1971)
(Civil Engineering)

McMaster University
Hamilton, Ontario,
Canada.

TITLE: Effect of Repeated Cyclic Lateral Loads on Load Bearing Shear Wall Panels

AUTHOR: D.J. de LISLE, B.E.,(HONS.) University of Canterbury, New Zealand.

SUPERVISOR: Dr. A.C. Heidebrecht

NUMBER OF PAGES: xi, 107

SCOPE AND CONTENTS:

The slitted wall, a concept originally used to improve the properties of infilled wall panels, is applied to shear wall structures. An ordinary reinforced concrete wall and three slitted walls were tested under cycles of repeated lateral displacements. The effect of vertical load and the lengthening of the slits to full panel height was also investigated.

The walls are compared by considering the different crack formations, stiffness deteriorations, load-deflection characteristics and energy properties. It is shown that

vertical slits do not produce improvements to the lateral response of wall panels. The application of vertical loads is beneficial and the lengthening of the vertical slits to full panel height is detrimental to the behaviour of the wall panels.

ACKNOWLEDGEMENTS

I wish to thank my supervisor, Dr. A.C. Heidebrecht, for his assistance throughout the course of this work.

I would also like to thank the technical staff of the Applied Dynamics Laboratory for their advice and help during the experimental investigation.

My thanks are also due to the Steel Company of Canada for supplying the reinforcing steel and to the Muto Institute of Structural Mechanics for supplying reference 19.

I would like to thank Mrs. Linda Frost for typing this thesis in its final form.

This experimental investigation was made possible through the financial assistance of the National Research Council of Canada.

TABLE OF CONTENTS

LIST OF FIGURES

LIST OF TABLES

CHAPTER I

INTRODUCTION

1.1 Shear Wall Structures

The shear wall, in its various forms, is now accepted as an economical form of constructing high-rise buildings. The design of multistory structures has reached the stage where the position and shape of the shear walls are governed by both architectural and structural requirements[1]. Architecturally the shear wall is used to divide and enclose space in a building, to enclose lifts, stairs and service ducts and to act as a barrier for noise and fire. Structurally the shear wall is used to transfer the various applied loads through the foundations to the ground.

The multistory structure can be divided into two main categories according to the functional requirements[2]. The first category contains the 'office building' which requires large open floor spaces for flexible office layouts to meet the needs of the various occupants. The shear walls for this type of structure tend to be grouped around the core area containing the lifts, stairs and utilities, and around the perimeter of the building.

The second category contains the high-rise apartment buildings. For this structure the shear walls are used as partition walls between apartments as well as around the service core and exterior walls.

The integrated functions of the various types of shear walls and shear wall buildings are due to the efforts of designers to produce more economical structures, that is, to produce optimum designs. An optimum structural design is achieved when the structure is designed for gravity loads only while the stresses due to lateral loads remain within the normally allowable overstress of 24 to 33 per cent[3]. The utilization of architectural and structural components such as elevators and service shafts, fire protective diaphram walls to resist lateral loads is essential in order to produce an optimum design of a structure.

1.2 Loads on Shear Wall Structures

The main structural requirement of shear walls is the transfer of the applied loads to the ground. The applied loads can be subdivided into two groups: dead loads and live loads. The dead loads are considered to be those whose effects are always present on the shear walls and they consist of the dead weight of the structural components, the architectural fittings and the mechanical services. The live loads consist of the effect of storage of goods, movement of people and vehicles, wind and seismic ground disturbances. By far the most important in the layout and in the structural design of shear walls is the effect of the horizontal live loads, that is, wind and earthquake loads.

In seismically active areas the effect of earthquakes on structures is of greater concern than the effect of wind, due to the lack of sufficient data from which reliable predictions on occurrence and likely strength of seismic ground motions can be made. The generally accepted earthquake resistant design philosophy (wind resistant design follows similar reasoning) considers moderate earthquakes to be resisted by elastic deformations of the structure and the more severe, but less frequent, seismic ground disturbances are to be resisted by the structure yielding locally into the inelastic range of the material. Under no circumstances can collapse of any portion of the structure be tolerated.

1.3 Elastic Behaviour of Shear Walls

The first part of the earthquake design philosophy states that for the frequently occurring seismic ground motions the lateral loads are resisted by the elastic deformations of the structural components. The elastic analysis of shear walls has interested many investigators over the last two decades and there now exists a number of different methods of solution. Shear walls without openings can be analysed as simple cantilever beams while the analysis of shear walls with openings, which are the more common type in practical buildings, can be carried out by three different methods.

1.3.2 Shear Connection Method

The first method considers the connecting beams of the coupled shear wall to be replaced by an equivalent continuous medium. This method was initiated by Chitty and developed and refined by Beck[4] and Rosman[5]. It assumes that the connecting beams have points of contraflexure at mid span and that the beams do not deflect axially so that a single second order differential equation can be formed. This equation has been solved for a number of different combinations of wall size and loading conditions and the results have been presented in graphical form applicable to practical design cases[6].

1.3.3 Column Frame Method

The second method uses the equivalent frame analogy and considers the coupled shear wall system to be replaced by line members representing the various structural elements[7]. The length of the connecting beams is taken as the distance between the centroidal axes of the adjacent columns. To account for the influence of the wall width on the connecting beams the portion between the ends of each beam and the centroidal axis of the wall is considered rigid. If the connecting beams are modified to be flexible over the total span between column axes, standard computer framework programs can be used for the solution of this problem[8].

1.3.4 Panel Element Method

The third method which is known as the panel element method has not gained acceptance as a practical engineering design tool. The finite element technique, using both triangular and rectangular elements, has been used by several research groups to explain the elastic stress distribution in various types of shear walls. However, the panel element method seems to have no advantage over the shear connection method or the wide column frame method for estimating the deflection of walls with openings[9].

1.4 Inelastic Behaviour of Shear Walls

The second part of the earthquake resistant design philosophy deals with the inelastic behaviour of the structure. Little is known about the real behaviour of shear wall buildings under seismic ground disturbances and code authorities often place restrictions on the building of shear wall structures in areas of high seismicity. The restrictions in the earthquake load provisions of the 1970 National Building Code of Canada are expressed in two ways:[10]

1. The seismic force factor K, for shear wall buildings, is specified to be 1.33 compared with 0.67 for ductile moment resisting space frames.
2. Shear wall buildings are restricted to a height of 200 ft. in Zones 1, 2 and 3 although this restriction can be exceeded in Zone 1 if "the walls are designed with special provision required for their ductile behaviour".

Similar provisions are specified in the 1966 Code of the Structural Engineers Association of California (SEAOC), although the height restriction is set at 160 ft.[11]. The inclusion of these restrictions is due to the damage suffered by shear wall structures subjected to major earthquakes[12,13].

The authorities responsible for the code provisions have not yet had sufficient experimental evidence of the behaviour of shear walls in the post-elastic range to be able to adopt a more liberal approach to the design of shear wall buildings. It should be noted that the National Building Code of Canada permits departure from the height restrictions if it can be shown that the structure can withstand the appropriate design earthquake with ductility and energy absorbing capacity equivalent to that in a structure with a ductile moment resisting frame capable of resisting at least 25 per cent of the lateral load.

1.4.2 Analytical Investigations of Inelastic Behaviour of Shear Walls

The post-elastic behaviour of coupled shear walls has been analytically investigated by modifying the continuous lamina approach. Winokur and Gluck presented an ultimate strength design approach in which they assumed that the collapse mechanism has plastic hinges at the points of contact of the coupling beams and the shear walls, and at the bottom of each shear wall[14]. The analysis was carried out in two stages. In the first stage the ultimate moments of the coupling beams were determined while in the second stage the system was considered as a vertical cantilever subjected to the ultimate lateral load and the ultimate coupling beam moments acting at the floor levels. The main disadvantage of this method is that no indication is given of the amount of inelastic deformations the coupling beams have to undergo to achieve the collapse mechanism of the coupled shear wall. Paulay, to overcome this deficiency, used an elasto-plastic technique to trace the behaviour of a coupled shear wall structure through stages of incremental lateral loading till the ultimate strength was reached[15]. Paulay used the simplifying assumption that the laminas possessed bilinear elasto-plastic load rotation characteristics.

1.5 Experimental Investigations of Shear Walls

1.5.1 Reinforced Concrete Shear Walls

On the experimental side the number of studies carried out on shear walls and shear wall components in the post-elastic range is limited. The most extensive work in this area was carried out by Benjamin and Williams in the early fifties, but, unfortunately the effect of repeated loading was not included in the study. However a number of important conclusions were drawn from this investigation which are relevant to shear wall behaviour[16,17].

1. The location of the first crack, and the cracking load are independent of the amount, type and location of the panel steel.
2. Panel reinforcing produces an increase in ultimate load. As the amount of reinforcing increases, the number of cracks before failure increases and the individual width of each

crack decreases.

3. Vertical steel is more effective than horizontal steel. Some horizontal steel is desirable to control cracking.
4. The length to height ratio of the panel influences the behaviour of the wall. As the length to height ratio increases the load at the first crack or at the first major break in the load-deflection diagram approaches the ultimate load. The crack pattern changes from flexural cracking to diagonal cracking.
5. The prediction of wall deflection is difficult as the wall does not necessarily behave elastically due to plastic flow and the presence of shrinkage cracks. Ordinary strength of material's theory gives reasonable results.
6. Openings decrease both the strength and rigidity of wall panels.

1.5.2 Slitted Shear Walls

In recent years the Japanese have carried out a lot of valuable earthquake resistant design research and now high-rise structures are permitted in Tokyo, which is an extremely active seismic area. The first few multistory buildings in Tokyo are of a composite structure, composed of a steel frame and reinforced concrete infill walls. The displacement incompatabilities of the flexible steel frame and the initially highly rigid reinforced concrete walls is overcome by the introduction of a new concept in shear walls, the slitted shear wall [18,19,20]. The slitted shear wall is a reinforced concrete wall containing a series of vertical slits. The slits are normally filled with asbestos sheets and are complete breaks in the concrete and in the reinforcing bar arrangement. From the experimental program, Muto concluded that the slitted walls eliminated the usual deficiencies of monolithic reinforced concrete walls. The initial rigidities were reduced and consequently the resistance to the lateral load would be more evenly shared by the steel framework and the concrete infill walls. High ductilities were also shown to exist which would allow the structure to undergo large deformations.

1.6 Purpose of This Investigation

This thesis reports on an experimental investigation which set out to determine whether the slitted wall concept could be applied to reinforced concrete shear walls. The object of the study was to discover if the inclusion of vertical slits would improve the performance of the reinforced concrete shear wall.

Three slitted walls are compared with an ordinary concrete wall. The one-story, half scale, shear wall panels were tested under repeated cyclic loading. Two of the panels were also subjected to vertical loads. The region of post-elastic deformation was the main area of study and an assessment of the effect of including vertical slits in reinforced concrete shear walls was made by comparing the strength, stiffness and energy properties.

The most common type of shear wall in practical structures is the coupled shear wall. The coupling beams greatly influence the behaviour of coupled shear walls in both the elastic and inelastic range. However, for this investigation it was decided to concentrate on the effect of vertical slits on wall panels. Paulay has studied in great detail the problems associated with coupling beams in shear wall structures[21,22].

CHAPTER II

DESCRIPTION OF TEST SPECIMEN AND LOADING FRAME

2.1 Test Specimen

2.1.1 Scale and Wall Panel Dimensions

To be able to relate the experimental work to practical structures, the wall panels for this investigation were scaled from an idealized shear wall building. The ten story shear wall building is typical of many high-rise apartment buildings and consists of parallel shear walls spaced at 20 ft. intervals as shown in Figure 1. The one story test panels represent the lowest story of the shear wall building. Small flange beams are incorporated in the walls to produce a change of section and second moment of area. A similar effect is created by the floor diaphrams in the real structure.

A half size geometrical scale was chosen for this investigation for two reasons. In the first place a half size wall panel would enable standard materials to be used in the construction of the panels and secondly no consideration of scale effects would be necessary in the interpretation of the test results. Previous investigators found that scale effects are extremely difficult to separate from variations in the material properties[16]. The dimensions of the wall panels are shown in Figure 2.

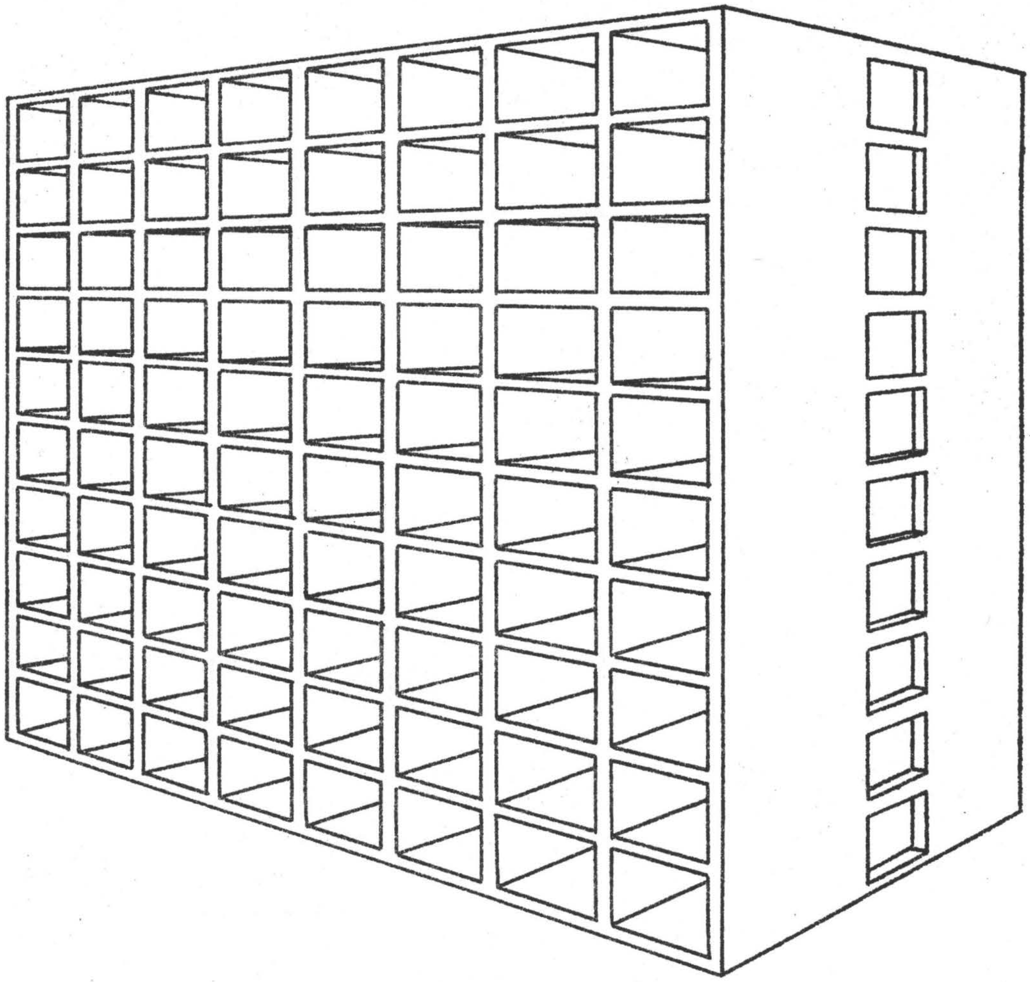

Fig. 1 IDEALIZED SHEAR WALL BUILDING

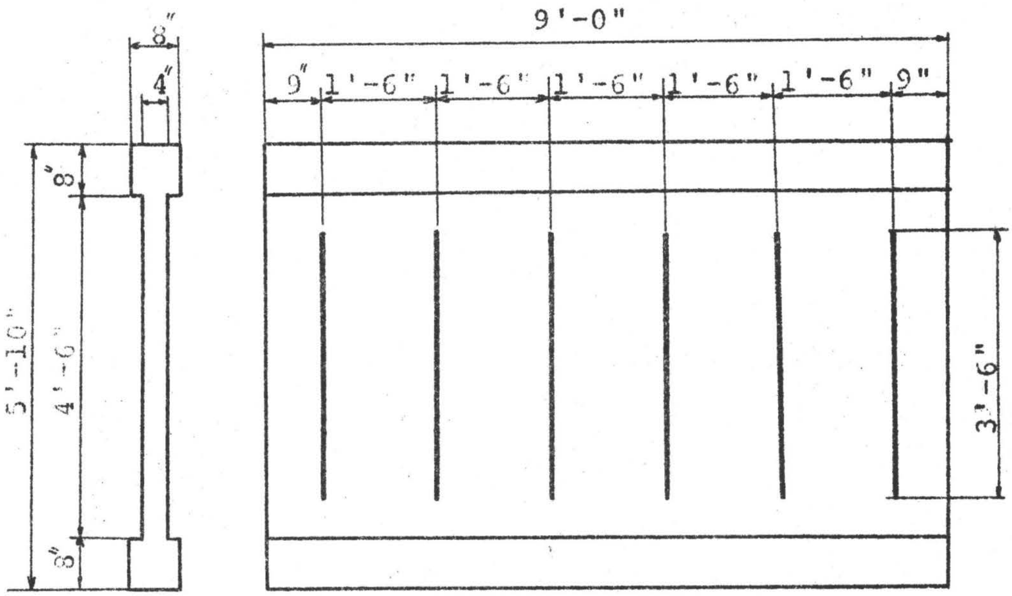

Fig. 2 DIMENSION OF WALL PANELS

2.1.2 Variables Investigated

A wide scatter of results can be expected from experimental investigations of reinforced concrete members, thus only one variable was altered in each panel. It was hoped that this system would permit constructive comparisons to be made between the four test panels.

The testing program was set up to investigate the following:

1. The behaviour of reinforced concrete shear wall panels under repeated lateral cyclic loading.
2. The effect on the lateral response of including vertical slits in reinforced concrete shear wall panels.
3. The effect on the lateral response of subjecting the reinforced concrete shear wall panels to vertical load.
4. The effect on the lateral response of lengthening the vertical slits to the full height of the panels.

2.1.3 Wall Panels

Four shear wall panels were tested in this investigation.

1. Panel A: the standard slitted panels
2. Panel B: the ordinary reinforced concrete wall
3. Panel C: the standard slitted panel
4. Panel D: the shear wall containing panel - high vertical slits.

The spacing of the vertical slits was chosen after a detailed study of the arrangements used by Muto[19]. Practical considerations were also involved in the final decision as a simple reinforcement arrangement consistent with construction practice was required.

2.1.4 Arrangement of Reinforcing Steel

An analysis of the structural system of the idealized shear wall building to a triangular lateral loading which represents a Zone 3 earthquake of the Canadian Code[11], showed that only nominal wall reinforcing was required. The arrangement of reinforcing was based on a value of 0.25 per cent of the gross section of the wall in both the horizontal and vertical directions[23,24]. The different steel reinforcing arrangements using No. 2 smooth bars are shown in Figures 3,4, 5 and 6. The flange beams were reinforced with four No. 2 bars in each corner and No.2 stirrups spaced at 9 in. centres.

2.1.5 Steel Reinforcing

No. 2 round bars (area ≈ 0.049 inches^2) were used for the steel reinforcing throughout the investigation. A series of three stress-strain tests were carried out to determine the properties of the reinforcing steel. The test specimens had an 8 in. gauge length and the strains were measured from two foil type strain gauges which were centrally mounted and 180 degrees apart. Two of the samples were subjected to a slowly increasing load and the load readings were recorded at strain intervals of 180 micro inches per inch. The stress-strain curves for these two tests are shown in Figure 7.

The third specimen was subjected to a series of repeated

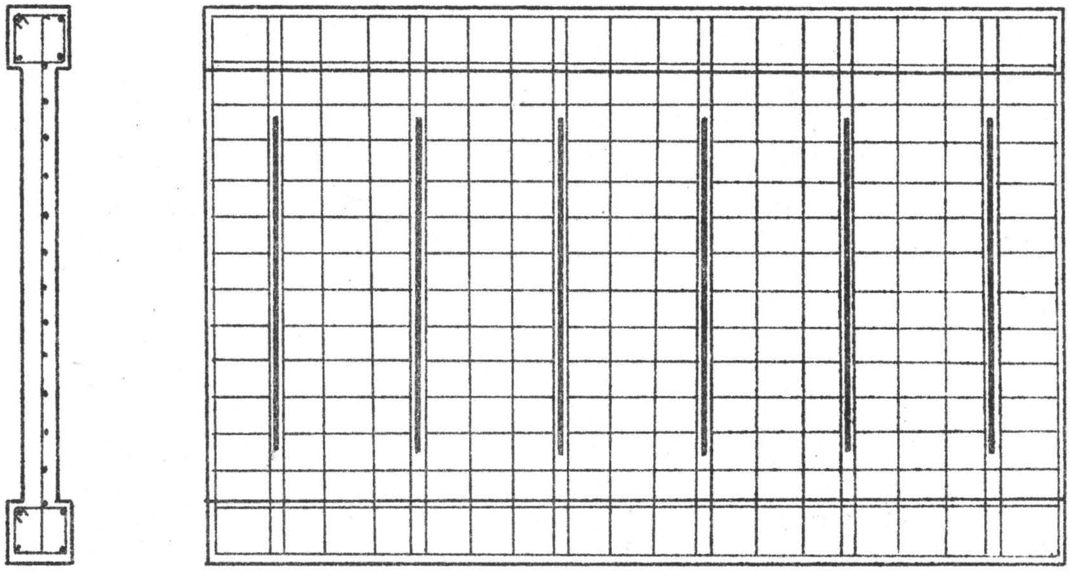

Fig. 3 REINFORCING ARRANGEMENT FOR PANEL A

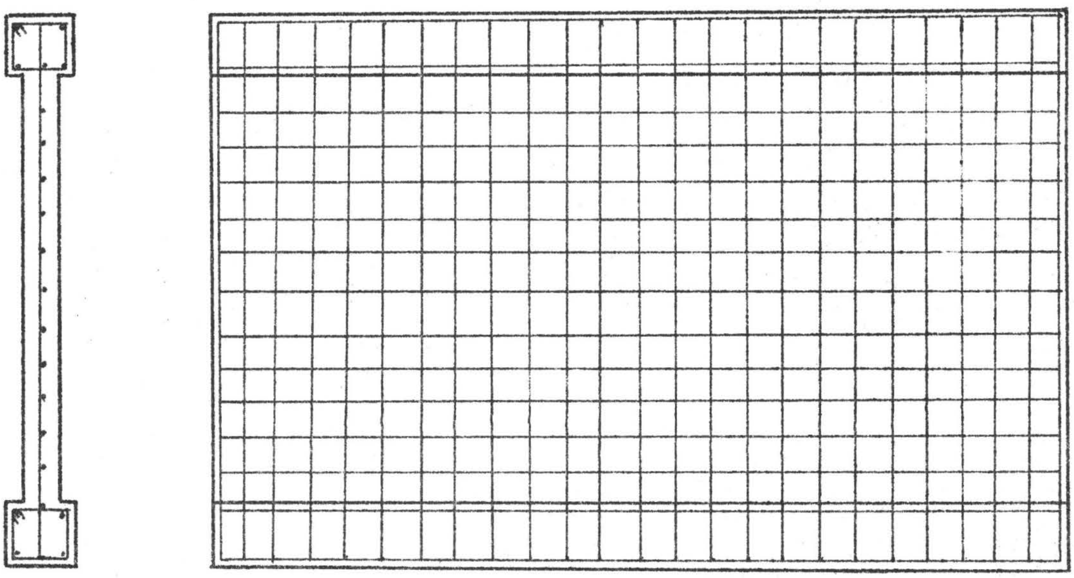

Fig. 4 REINFORCING ARRANGEMENT FOR PANEL B

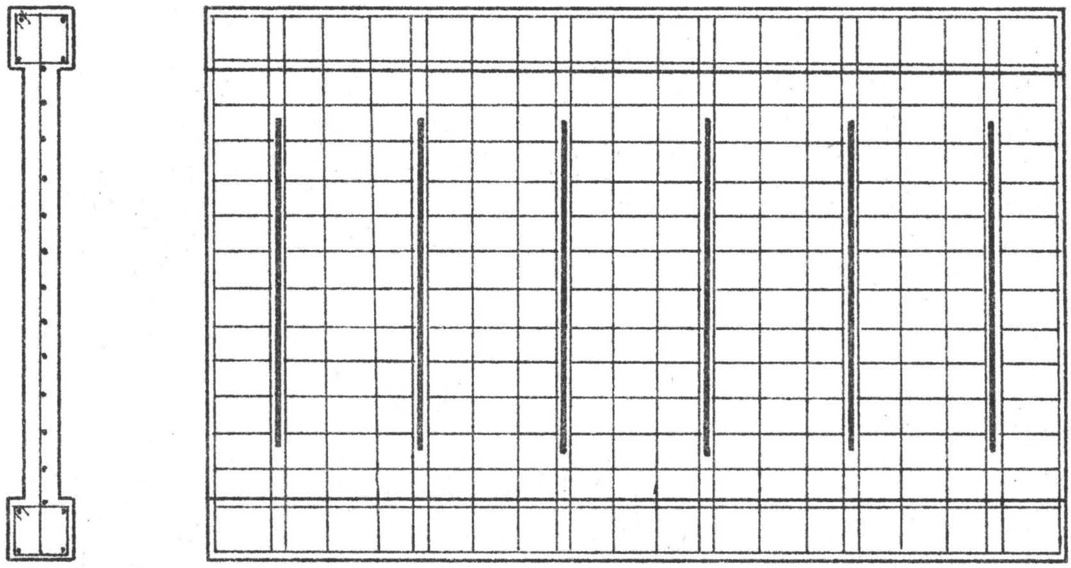

Fig. 5 REINFORCING ARRANGEMENT FOR PANEL C

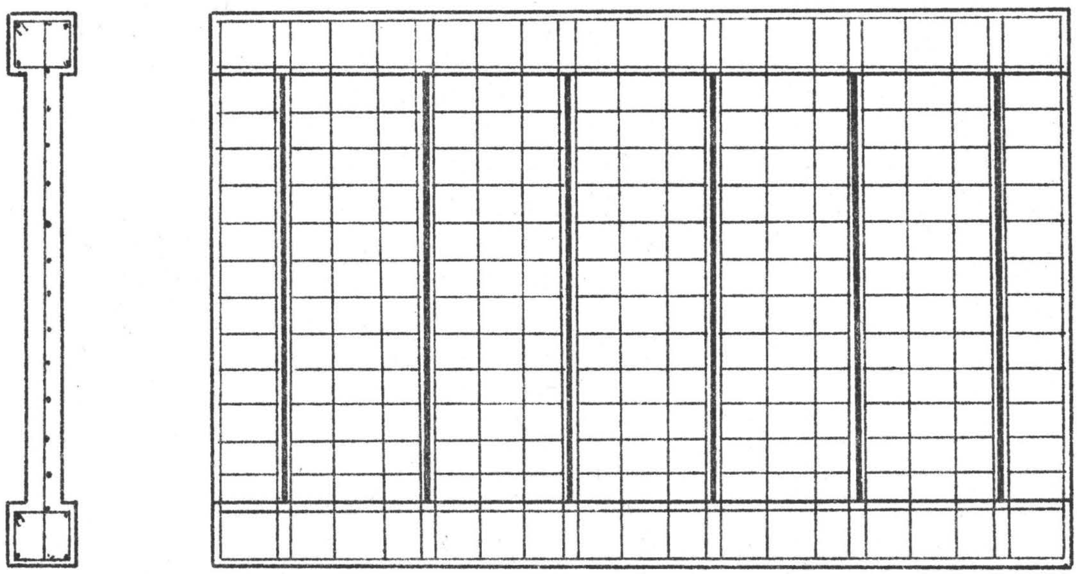

Fig. 6 REINFORCING ARRANGEMENT FOR PANEL D

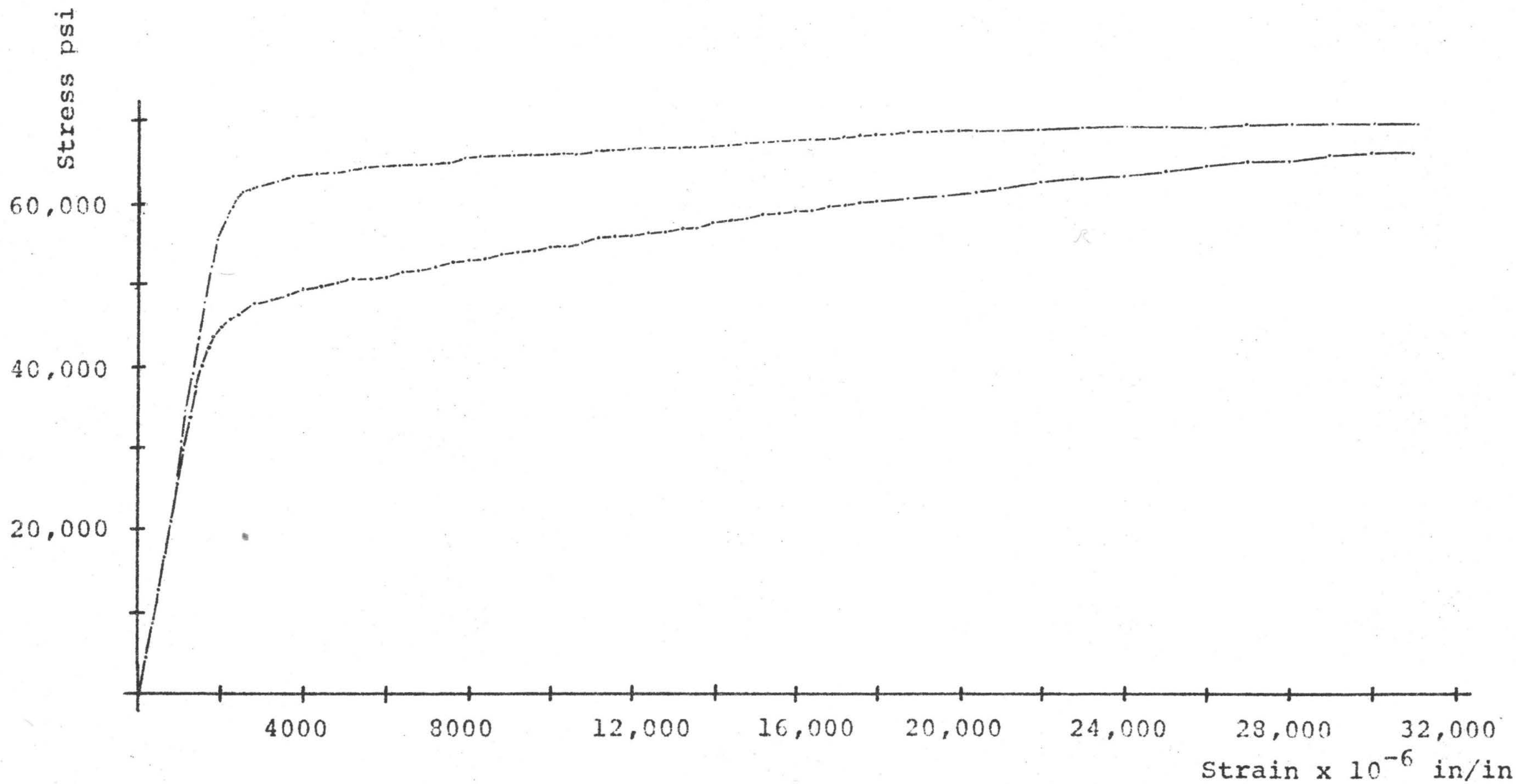

Fig. 7 STRESS STRAIN RELATIONSHIPS FOR REINFORCING STEEL

loads, a state which more nearly represents the actual conditions that occur in a reinforcing bar in a wall panel under repeated lateral cyclic loading. In the real case, at critical positions in a wall subjected to repeated lateral cyclic loading, a reinforcing bar would undergo some compressive strains after the tensile straining cycle. Unfortunately the small cross sectional area of the reinforcing steel did not permit compressive strains to be applied to the specimen. Consequently a full investigation of the Bauschinger effect was not possible. It was noted, however, that repeated plastic straining of the reinforcing steel caused a slight stiffening of the specimen. Similar effects have been reported in the literature(25). The stress-strain curve for the third sample is shown in Figure 8.

2.1.6 Concrete

A 3000 p.s.i. commercial, ready-mix concrete was used for the construction of the four shear wall panels. At the completion of each test four concrete cylinders were crushed to determine the ultimate compressive stress and the modulus of elastic of the concrete. A loading speed of approximately 0.05 in. per minute was used for the tests and the modulus of elasticity was determined using the secant modulus at a stress of 0.45 f'_c(26). A typical stress-strain curve of the concrete is shown in Figure 9 while the various properties of the concrete cylinders are displayed in Table 1.

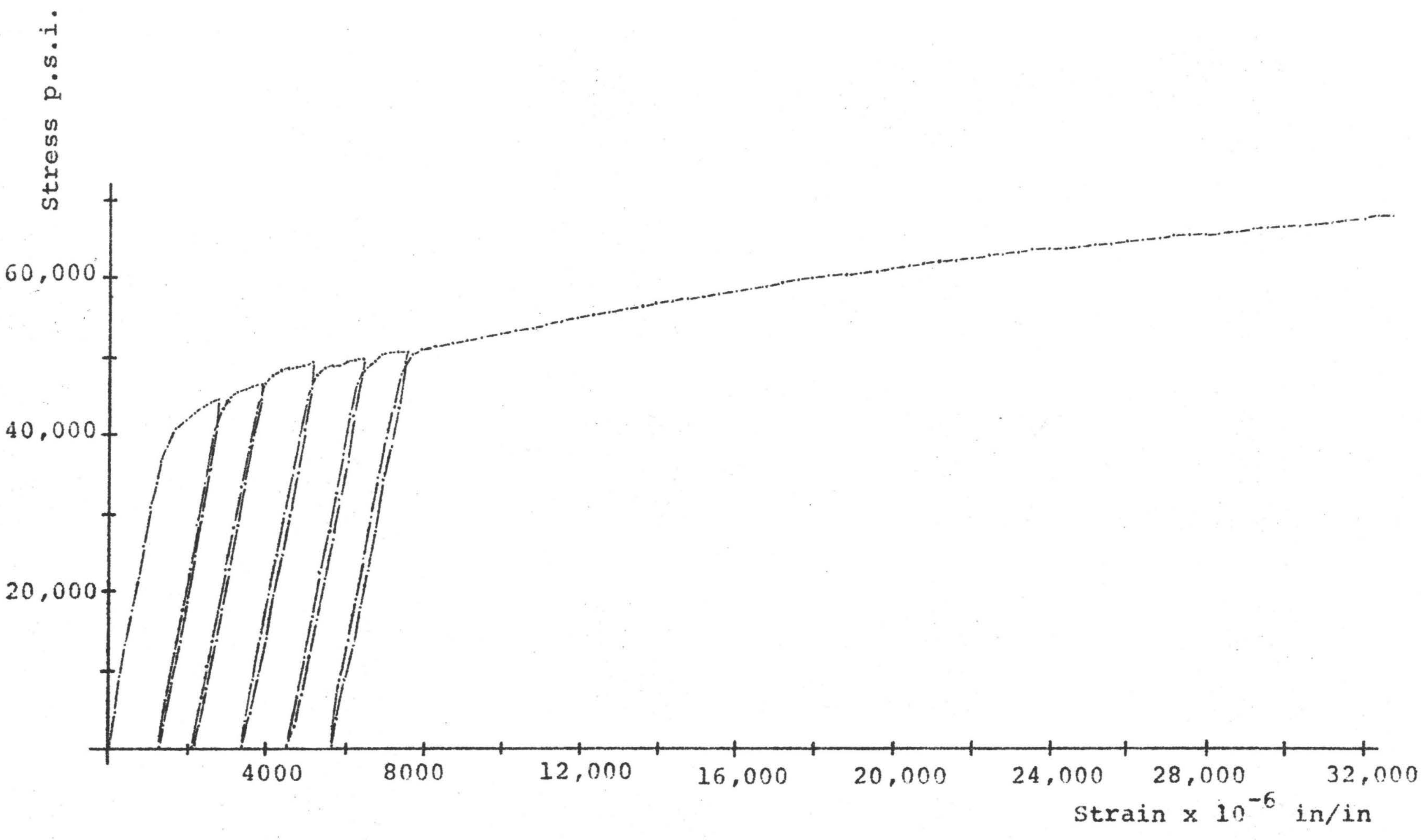

Fig. 8 STRESS-STRAIN RELATIONSHIP FOR REINFORCING STEEL

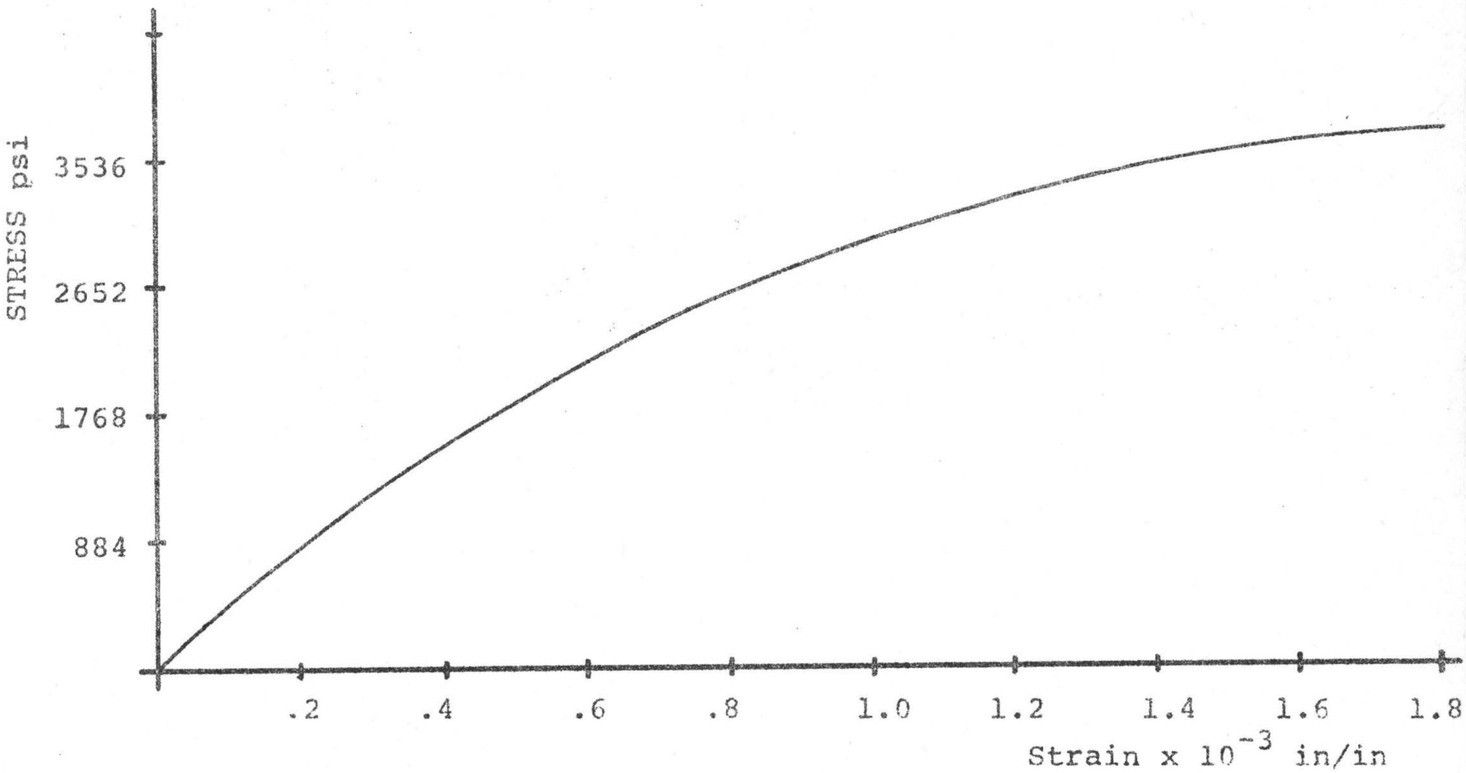

Fig. 9 TYPICAL CONCRETE CYLINDER STRESS-STRAIN RELATIONSHIP

CYLINDER	DENSITY lbs/cu.ft.	f'_c psi	ELASTIC MODULUS x 10^6 psi
A1	150	3780	NO STRAIN MEASUREMENTS TAKEN
A2	148	3470	
A3	147	3720	
A4	147	3800	
B1	147	3740	4.55
B2	144	3740	3.11
B3	145.5	3890	3.83
C1	144	3720	3.71
C2	147	3680	3.76
C3	147	3650	3.80
C4	144	3720	3.76
D1	143	3650	3.64
D2	143	3900	3.90
D3	148	4320	4.40
D4	147	3700	3.98

TABLE 1 CONCRETE CYLINDER RESULTS

2.2 Description of Loading Frame

2.2.1 Introduction

The four tests described herein are only the beginning of a long term project investigating the inelastic deformation behaviour and the energy properties of load bearing shear walls. The long term objectives are to establish design recommendations for reinforced concrete shear walls and to evaluate the suitability of various materials such as brick, concrete block and styrofoam sandwich panels for use as load bearing shear walls in seismic areas.

2.2.2 Basic Requirements of the Loading Frame

In the design of the apparatus for testing load bearing shear wall panels under lateral load three basic requirements were considered.

1. Panels of various materials and dimensions could be tested in the loading frame.
2. A reversible lateral load could be applied to the wall panels.
3. The wall panels could also be subjected to two constant vertical loads.

2.2.3 Review of Previous Experimental Methods

A review of the various experimental methods for testing shear walls was made before the design of the apparatus was finalized. Muto investigated the slitted wall concept by testing infilled panels under direct shear loading[19] while Paulay has proposed a testing arrangement which applies a shear force to the top edge and also a distributed moment to the panel[27].

The difficulty of applying large vertical forces to wall panels which undergo lateral displacement was noted. A method of surmounting this problem was used by Stafford Smith for the testing of brick infilled steel frames[28]. Two panels are constructed end to end and the vertical loads are applied through the sides while the lateral load is applied through the middle beam. The testing arrangement is shown in Figure 10. This method was considered unsuitable for the testing of load bearing shear walls for the following two reasons.

In the first place this type of test set up prevents the wall from deflecting to its true deformed shape. At low lateral loads and small displacements the panel deformations are essentially due to shear deflections and the apparatus used by Stafford Smith correctly reproduces these conditions. However for large displacements, especially if extensive cracking of the concrete and yielding of the steel reinforcing occurs, the bending deflection due to cantilever action becomes very important. The Stafford Smith test set up prevents this from occurring and as the main purpose of the investigation was to study the post-cracking behaviour of load bearing reinforced concrete shear walls this type of loading frame was not considered suitable.

Secondly the testing method was not feasible for half scale wall panels. A half scale specimen would have outside

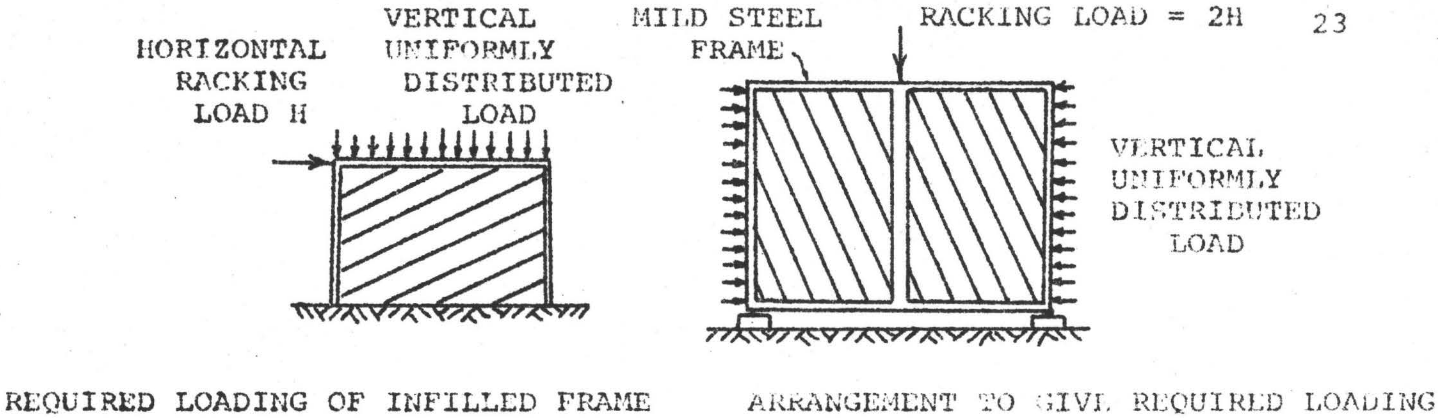

FIG. 10 STAFFORD SMITH'S TESTING ARRANGEMENT

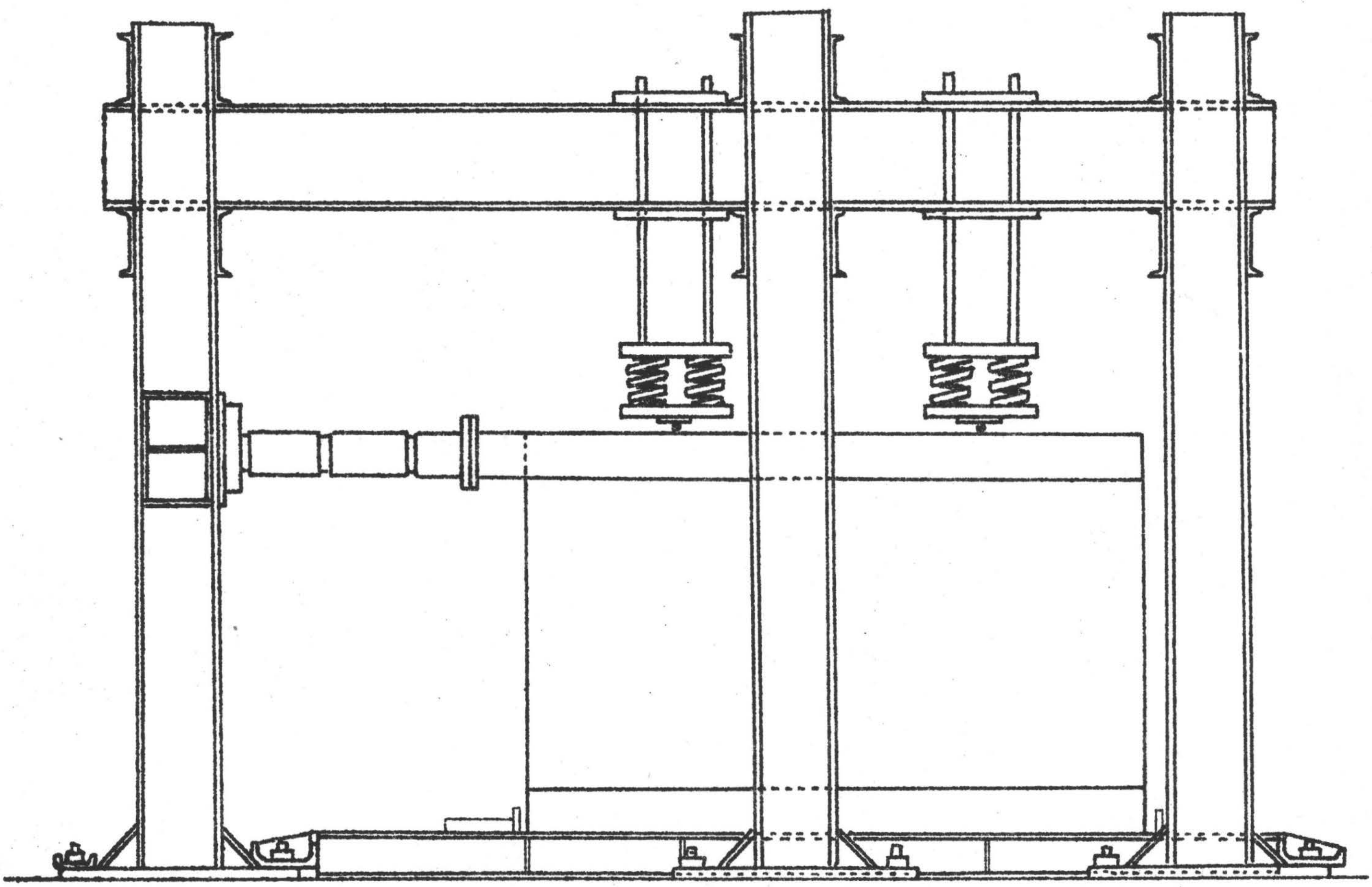

Fig. 11 LOADING FRAME

dimensions of 10 ft. by 9 ft. and such a model would not be manageable with the laboratory facilities available.

2.2.4 Loading Frame

The solution finally adopted for the loading frame was to test the half scale shear wall panels directly under lateral and vertical loads. A diagram of the apparatus is shown in Figure 11 and a general view of the test set up is given in Figure 12.

The main testing frame was built up from a series of 14" x 14" WF. columns secured firmly to the laboratory floor by pretensioning the base bolts. The 18" x 7 1/2" x 5/16" WF. vertical loading beam was attached to the columns through twelve 12" x 3" x 3/8" channels. The connections between the beam and the channels, and the channels and the columns were made by 1" diameter black bolts.

An 8" x 8" x 3/8" WF. base beam was connected to the main test frame by two 12" x 3" x 3/8" channels and secured to the floor at the left hand end by a 10" x 10" RHS. At the right hand end two 15" x 3" x 3/8" channels were bolted to the columns to prevent vertical movement of the base beam.

2.2.4.1 Lateral Loading System

A 250 kip capacity actuator was used to supply the lateral load to the shear wall panels. The actuator is hydraulically operated by a servo value and is controlled through the Material Testings Systems (MTS) Console. The MTS Console is able to control the actuator by either displacement or load.

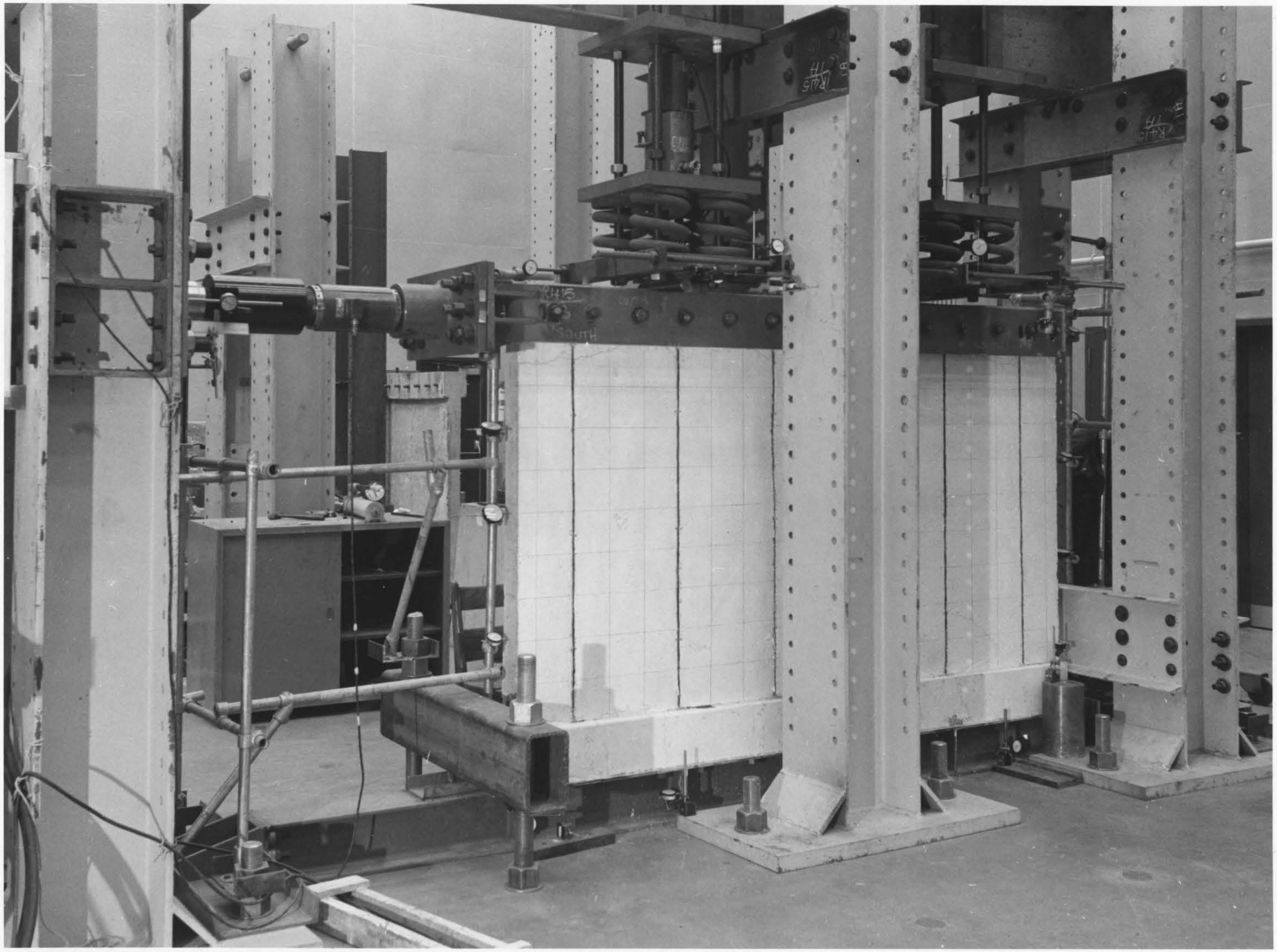

Fig. 12 PANEL D IN LOADING FRAME

The method of connecting the actuator to the left hand set of columns is shown in Figure 13. Four stiffening boxes were constructed from 1/2 in. plates to fit within the flanges of the columns to prevent buckling under the high reaction forces set up by the actuator. Two 3/4 in. plates were bolted to the flanges of the columns and the actuator was connected to these plates by four 2 in. diameter bolts. One end of a 250 kip capacity load cell was threaded into the actuator while the other end was threaded into a specially constructed connection piece.

As mentioned previously one of the basic requirements of the loading frame was the reversibility of the lateral load. This was achieved by a loading yoke which consisted of two 1 in. thick plates, 8 in. wide and 9 ft. 6 in. long. The plates were bolted to the sides of the upper flange beam of the shear wall panels by a series of 1 in. diameter threaded rods cast into the concrete. The loading yoke was connected to the actuator through twelve 1 1/4 in. diameter bolts at the specially constructed connection piece.

The method of securing the lateral loading yoke to the wall panels was used to simulate the transmission of lateral load through the floor systems of a building subjected to seismic ground motions. Earthquake ground motions cause accelerations of the buildings masses which are essentially concentrated in the floor systems.

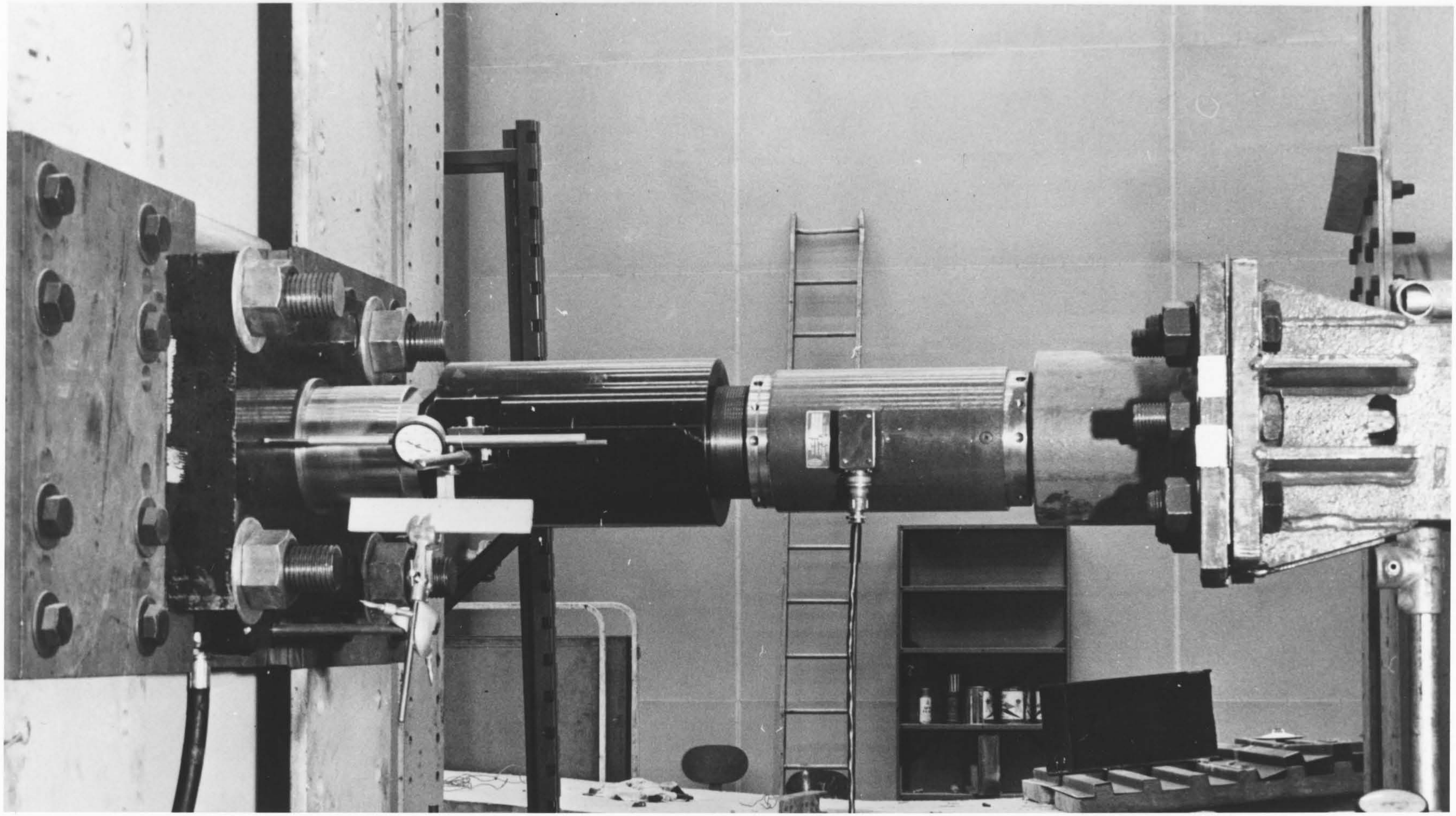

FIG. 13 CONNECTION METHOD FOR HORIZONTAL ACTUATOR

2.2.4.2 Vertical Loading Systems

The vertical loading systems employed the basic principles of an apparatus used to evaluate the creep of reinforced concrete members. The vertical loading system is shown in Figure 14. The loading system was made from four 2 in. thick steel plates and four 1 1/2 in. diameter threaded rods. Four stiff springs were included in the loading system to minimize the change of load due to vertical movement of the wall panel. A spring constant of 13.5 kips per inch was specified for the manufacture of the springs.

Several methods were tried for transferring the load from the vertical loading system to the shear wall panel. The most successful was a polished round bar between a smooth steel plate and the polished channel section cast into the top flange beam of the wall panels. This system was used for panels C and D.

The movement in the horizontal directions due to the friction effects was restricted by a bracing system which was bolted to the columns of the loading frame. The bracing rods were pretensioned by firmly tightening the nuts at the column flanges.

2.2.5 Instrumentation

The output data required from the series of four tests was in the form of the applied lateral load and the corresponding deflection, and the deflected shape of the shear wall panel. No strain measurements on the concrete panels were

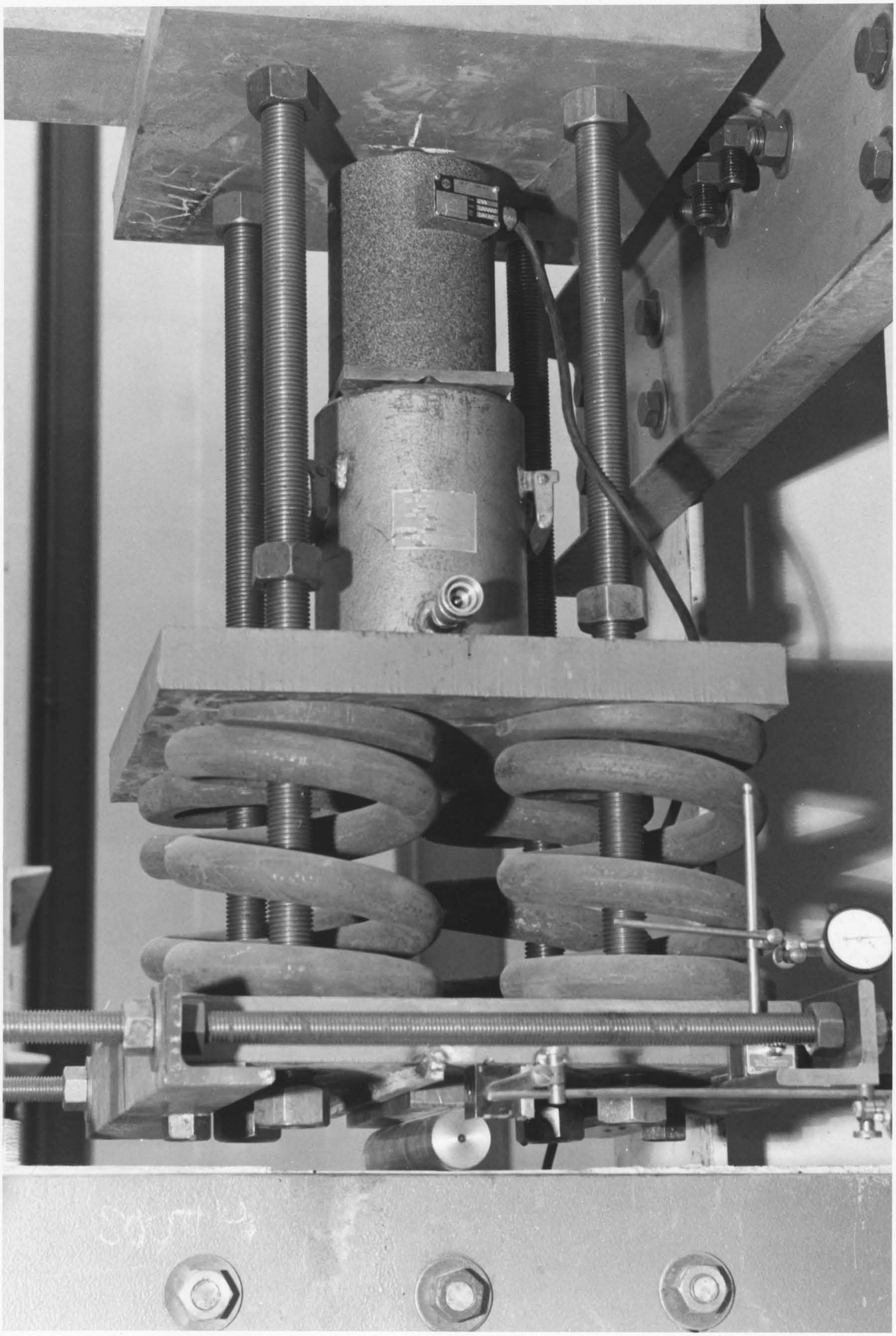

Fig. 14 VERTICAL LOADING SYSTEM

recorded as most of the load cycling took place after cracking, where strain readings are difficult to interpret.

A tubular framework was constructed around the wall panel in the loading frame. The arrangement of the tubular frame is shown in Figure 12 while the positions of the dial gauges for the four tests are shown in Figures 15 and 16. The dial gauges were positioned to record:

1. The deflection along the line of application of the lateral load.
2. The deflected shape of the shear wall panel.
3. Movement perpendicular to the plane of application of the lateral load.
4. Vertical and horizontal movement of the base beam.
5. The amount of movement of the actuator.

In the third and fourth tests additional dial gauges were included to measure the vertical and horizontal movement of the vertical loading systems.

The load from the horizontal actuator was measured by a 250 kip capacity load cell. The voltage from the load cell was displayed on a digital voltmeter which was also able to display the voltage from the linear voltage displaced transducer (LVDT). The LVDT was positioned to measure the displacements of the horizontal actuator.

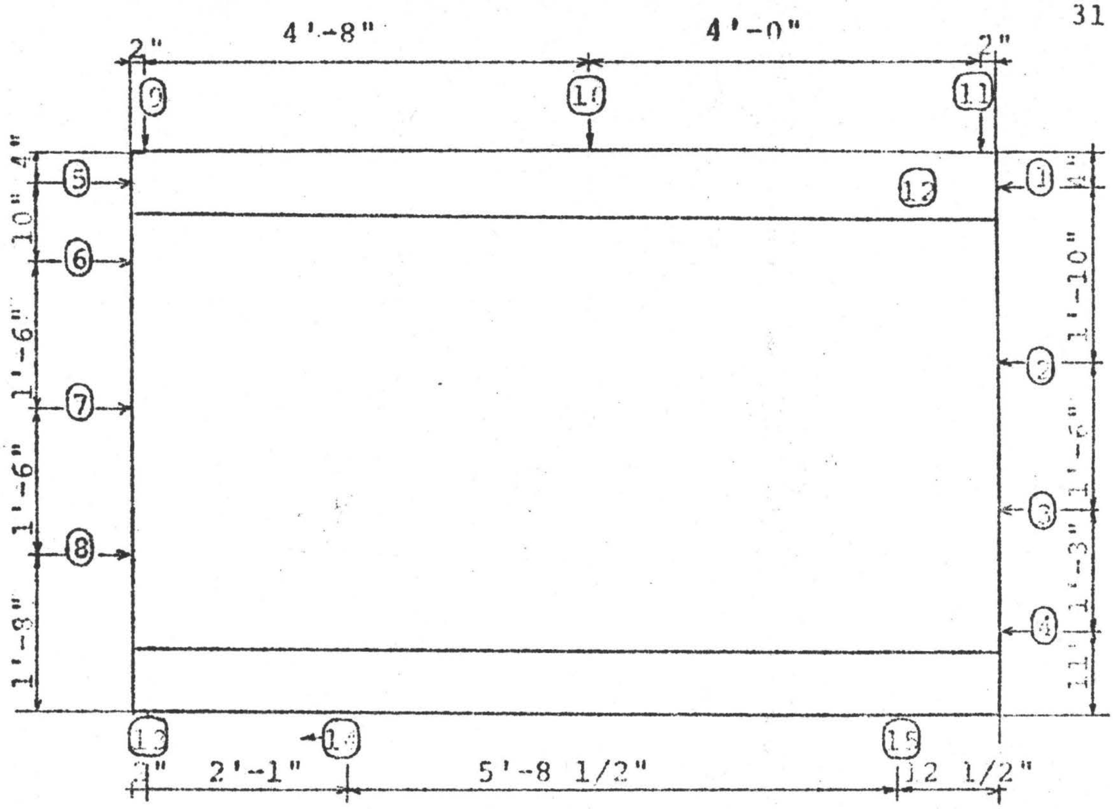

Fig. 15 DIAL GAUGE POSITIONS FOR PANELS A AND B

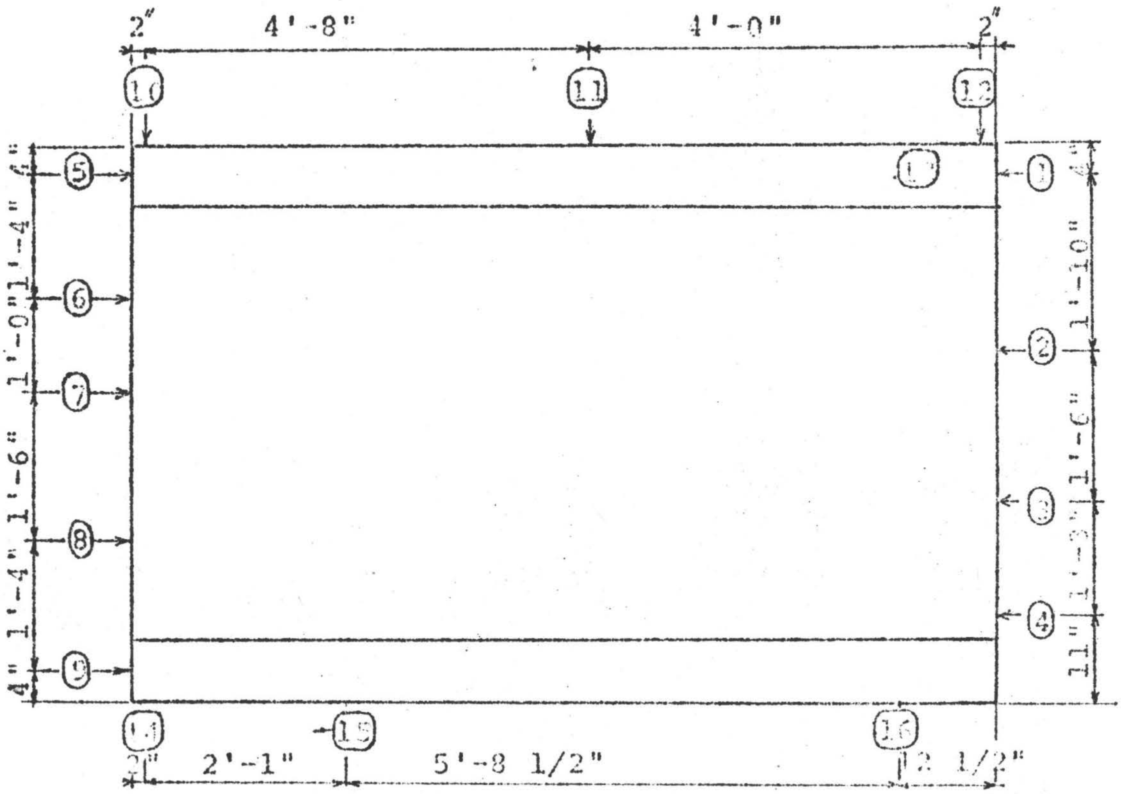

Fig. 16 DIAL GAUGE POSITIONS FOR PANELS C AND D

CHAPTER III

PREPARATION OF SPECIMEN FOR TESTING AND THE TESTING PROCEDURE

3.1 Preparation of Specimens for Testing

The preparation of a shear wall panel began with the assembling of the formwork. The bases of the forms were constructed from 5/8 in. plywood and were stiffened by 2" x 2" battens. Steel channels provided the necessary rigidity to withstand the large pressures imposed by freshly poured concrete. Holes were drilled in the plywood base and in the steel channels for the accurate placing of the 1 in. diameter threaded rods. The forms were set up as shown in Figures 17 and 18 and the walls were poured in that position.

For the first two wall panels (Panels A and B) the reinforcing mats were built using wire to secure the various bars. However, for Panels C and D spot welding was used to form the reinforcing mats as great difficulty was experienced in securing the small horizontal pieces to the vertical rods with wire in Panel A.

The reinforcing mat was centrally located in the formwork by placing it on a series of wire seats formed from No. 2 bars. The 4 in. wide strips of asbestos were held in position by No. 2 rods pushed into specially prepared holes in the plywood base. These pegs were removed as soon as the amount of

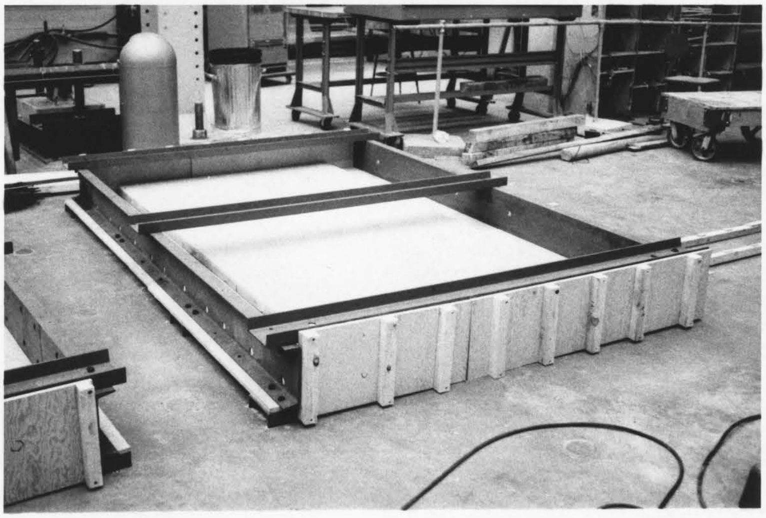

Fig. 17 FORMWORK

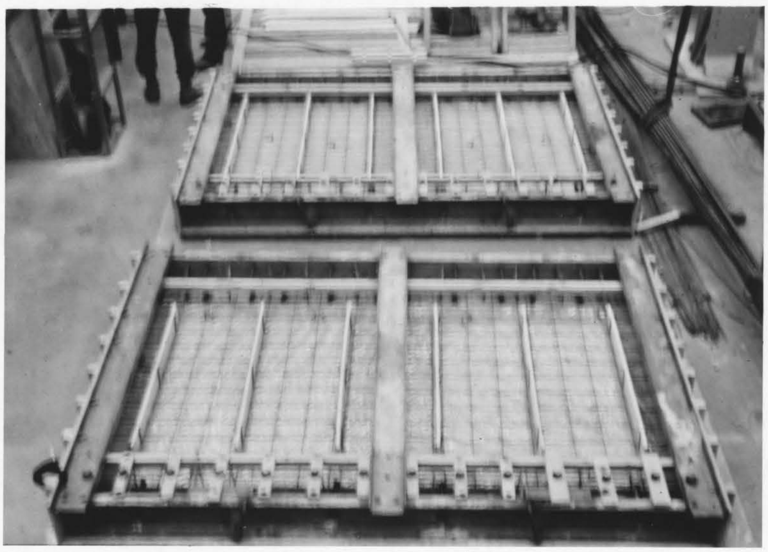

Fig. 18 PANELS C AND D READY FOR POURING

newly poured concrete was sufficient to prevent movement of the 1/2" thick asbestos strips.

The 1 in. diameter threaded connection rods were placed in the specially prepared holes in the top and bottom flanges. Additional rigidity was provided for the threaded rods by tying the rods into the reinforcing mat.

To prevent the concrete from adhering to the plywood base and sides a thin coating of oil was applied to panels A and B prior to the pouring of the concrete. This method was changed for the last two panels where a plastic sheet was laid across the base of the formwork. This technique proved highly successful as the time for the stripping of the formwork was reduced by a factor of four.

1 3/4 cubic yards of concrete were required to pour two panels simultaneously. A standard 3000 p.s.i. commercial ready-mix concrete with a specified slump of 2 in. was ordered. A 1/2 in. deviation from the specified slump was considered acceptable. Four 6 in. diameter cylinders were prepared for each panel using a vibrating technique for compaction.

The panels were cured under damp burlap for three days. The forms were then removed and the panels were stored in the upright position in a specially constructed storage craddle.

The panels were manoeuvred into the testing position through the side of the loading framework in a series of three moves. The panels were positioned vertically by shims and bolted securely to the base beam. The gaps between the stops on the base beam were carefully filled in with steel blocks. The loading yoke was manoeuvred into position and tightly bolted to the sides of the upper flange beam. The coupling between the loading yoke and the horizontal actuator was made through the specially constructed connection piece. For panels C and D the top bearing channels, cast into the upper flange beam, were sanded to provide a smooth surface for the round bar of the vertical loading system to bear on.

The front surface of panels A and B were covered with a coat of white-wash while white paint was used for panels C and D. The change was made to overcome the difficulty of applying an even coat of white-wash. A 6 in. grid system was marked on the white surface and the asbestos slits were painted black to enable the crack formations to be easily identified.

3.2 Testing Procedure

3.2.1 Lateral Loading Sequence

A study of the various strong motion earthquake records currently available reveals the completely random nature of a seismic ground motion. The present state of the art does not permit the prediction of earthquakes or seismic ground motion records. Consequently the exact behaviour of a structural component during an earthquake cannot be determined by experimental methods. However, if tests are carried out under similar conditions to those imposed by earthquakes it is possible to assess the reliability and the behaviour of the component to earthquake type loading.

In the testing of seismic resisting components two approaches have been used. The loading cycles can be chosen to represent the motion of a possible earthquake[29], or they can be repeated at the same control parameter a number of times before moving to the next cycling position[30]. For the four tests of this investigation the second approach was adopted. It was felt that this method would provide more information about the various properties that are affected by load cycling in the post-elastic region. Also in the first method the exact values of the control parameters are difficult to ascertain during the portions of violent ground motion.

3.2.1.1 Displacement Control

The horizontal actuator was controlled by displacement to enable a detailed investigation of the inelastic deformation of the wall panels. Horizontal displacement control permits an accurate study of the behaviour of the reinforced concrete member around the failure region. Failure is considered to occur when there is a significant load reduction with further displacement. A load control system prevents the failure region from being accurately determined.

The sequence of lateral loading consisted of thirteen displacement cycles. The different displacement positions were chosen so that the range from zero displacement to failure could be studied. The first twelve cycles were divided into four displacement positions and three lateral cycles were carried out at each displacement position. The initial series of three cycles was to determine the elastic properties of the wall panels while the remaining three sets were spread throughout the inelastic region. In the final cycle the wall panel was displaced as far as the loading frame would permit.

The aims of the sequential lateral displacement cycles were to assess the effect of repeated lateral cycling on the stiffness and energy properties of the wall panels and to evaluate the effect on these properties of cycling at the same displacement.

3.2.2 Data Recording

The maximum displacement position for each cycle was divided into approximately thirty points. At each incremental displacement point, load and displacement readings were recorded. During the period of time required to record the various measurements fluctuations occurred in these readings. Efforts were made to correct this fault but only a small improvement was achieved. It was thought that the fluctuations were due either to the hydraulic pumping system or to the electronic systems of the MTS console. Initial and final values of all critical measurements were taken as no solution to this problem was available.

The fluctuations of the actuator prevented any study of the effects of creep on the wall panels or an evaluation of the build up of residual loads during a complete test. Each lateral displacement cycle was carried out as a completely separate test. Initial readings were taken and the relative values of load and displacement were calculated from them. The average time of testing for a single cycle was about three hours while the time between cycles varied from 0 to 2 days.

3.2.3 Vertical Loads

Panels A and B were tested under lateral load only while for panels C and D two vertical point loads were also applied. The value of the vertical load was determined by considering the idealized shear wall structure of Figure 1 to be subjected to full dead load + one-third live load, making a total vertical load of 600 kips. Instead of applying the geometric scale factor to the loads the vertical stress of the half scale wall panel was made equal to that of the full size wall. The value of the load for each vertical loading system was 75 kips.

In coupled shear wall structures lateral displacements cause changes to occur in the values of the vertical load. However, since the purpose of this investigation was to concentrate on the behaviour of the wall panels under lateral loading the effect of coupling beams was neglected.

The vertical loads were applied before the start of the lateral displacement cycles. During the test the left hand end loading system was monitored by the load cell and an actuator (see Figure 12). At the beginning of each new incremental lateral displacement point the load was returned to the specified value of 75 kips. The right hand end loading system was monitored by a dial gauge as no means existed of altering the load without transferring the load cell and actuator from the left end system to right end system. The right hand end load was restored twice during each test.

3.2.4 Search For Cracks

At each incremental displacement point a search for new cracks was undertaken. New cracks were marked on the face of the wall panel and the load at which they occurred was recorded. An extensive photographic record was kept of the formation of cracks in the four panels.

CHAPTER IV

PREPARATION OF RESULTS

4.1 Reduction of Results

In the section on testing procedures, it was noted that fluctuations of load and displacements occurred during the time required to record all the values. For all the result calculations, the average of the initial and final measurements were used. The displacement along the line of application of the load was taken as the average of the average values recorded at each end.

A rotation reduction was carried out on all displacement values as the rotation of the base beam was too great to ignore. The base beam was assumed to remain perfectly rigid between the two points where the vertical displacements of the base beam were recorded. It was further assumed that the wall rotated through the same angle as the base beam.

4.2 Friction Forces

For panels C and D a series of tests were carried out to determine the values of the frictional forces induced at the contact surfaces of the vertical load rollers and the bearing plates of the wall panels. The vertical load was applied only at the left hand end load point and it was varied between 0 and 75 kips. At each vertical load setting the wall panel was laterally displaced and the load and deflection readings were recorded. The load readings were reduced so that at the initial position the load value was zero. From the reduced results, load-deflection curves were drawn for each vertical load setting and the load values for a set of horizontal displacements were read from these curves. The additional horizontal loads ΔP, required to displace the wall panel a distance ΔX, were calculated for the various vertical load settings. It was assumed that the additional load ΔP was made up of two components, the first component being the frictional force induced by the vertical load rollers and the second component being the lateral force required to overcome the stiffening of the panels due to the application of the vertical loads. It was further assumed that the frictional force in the rollers was constant. For each vertical load setting a curve of ΔP versus horizontal displacement was drawn. The resulting straight line curves were projected back to the ordinate axis and the intercept was read off as the frictional force. A fair amount of scatter of the plotted results was experienced so an average value was used. In Figure 19 and 20 a set of graphs are presented that were used to determine the frictional forces in panel C. The frictional force values of 0.3 kips per load point is small and any inaccuracies in the assumptions and calculation method would not greatly effect the trends in the results.

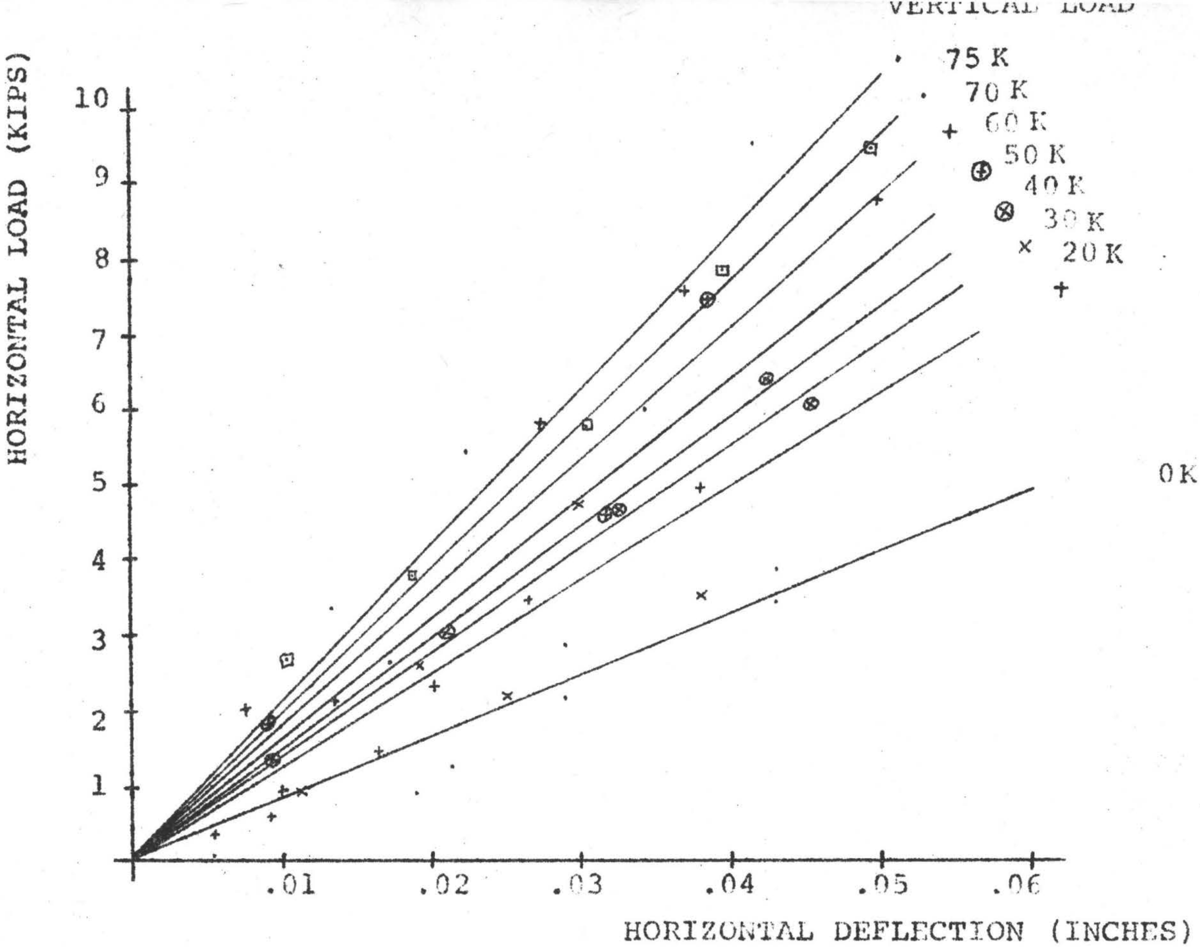

Fig. 19 FRICTIONAL FORCE DETERMINATION FOR PANEL C

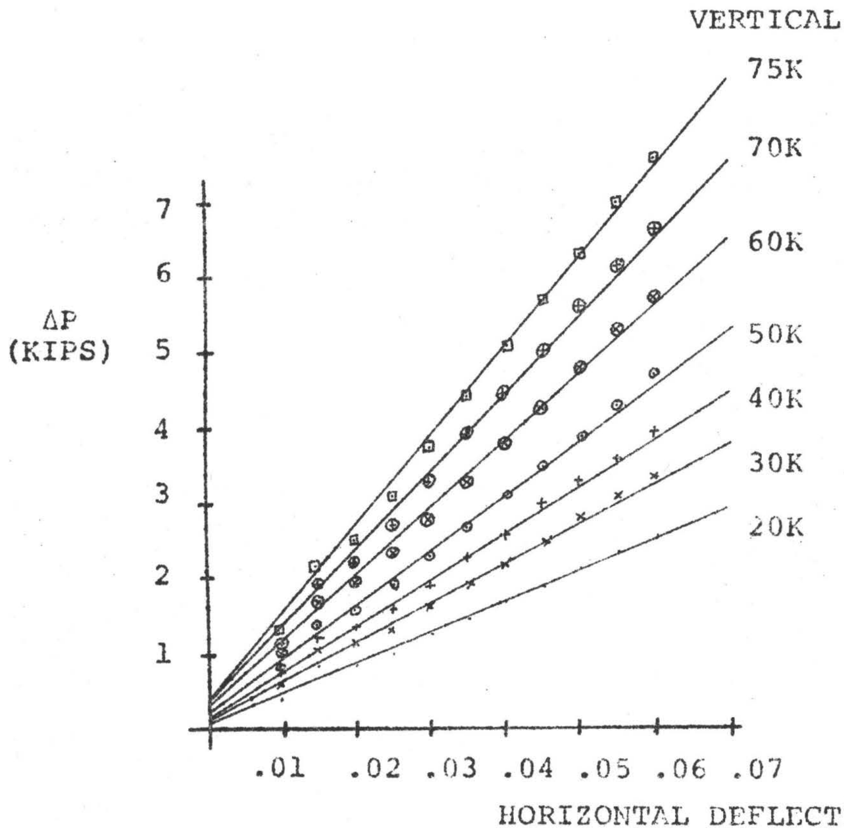

$\Delta P_i = (P_N - P_o)_i$

= Horizontal Force Required for Displacement i with Vertical Load N minus Horizontal Force Required for Displacement i with zero vertical load

ASSUMPTIONS:

A. $(P_N - P_o)_i$ has two components

1. Due to Frictional Forces in Rollers
2. Due to Stiffening of Panel Effect from Vertical Loads

B. Frictional Force Constant

Fig. 20 FRICTIONAL FORCE DETERMINATION FOR PANEL C

4.3 Drawing of Graphs

In the graphical presentation of the results it is desirable to include on one diagram the effect of deflections and the number of lateral cycles on the various properties of the wall panels. This is achieved by using the average deflection multiplied by the square root of the number of cycles along the abscissa axis. There exists no scientific basis for the selection of this procedure.

4.4 Energy Calculations

The energy properties of the wall panels were calculated from the load-deflection diagrams. The area under the load-deflection curves represents the energy absorbed by the wall panels while the area within the hysteresis loops represent the energy dissipated by the panels.

CHAPTER V

FORMATION OF CRACKS

5.1 Introduction

The formation of cracks in reinforced concrete members is extremely difficult to predict. It has been shown that micro-cracking exists, due to a number of causes, even before the external loads are applied[31]. Consequently the behaviour of reinforced concrete is never truly elastic. However, it is generally considered that the elastic principal stress concept can be applied to reinforced concrete members before visible cracking occurs[32,33]. The elastic principal stress concept is used in this investigation to explain the position of the formation of the initial cracks.

5.2 Elastic Principal Stresses

Before visible cracking occurs, it is assumed that all the wall panels behave as elastic, homogeneous, isotropic materials. By calculating ϕ, the direction of the principal stresses, for a number of points within a cantilever beam acted upon by a point load at its end, it is possible to construct the stress trajectories for the wall panels. The stress trajectories are defined as the two families of orthogonal curves whose tangents at each point coincides with the directions of principal stress at that point[34]. Figures 21 and 22 show

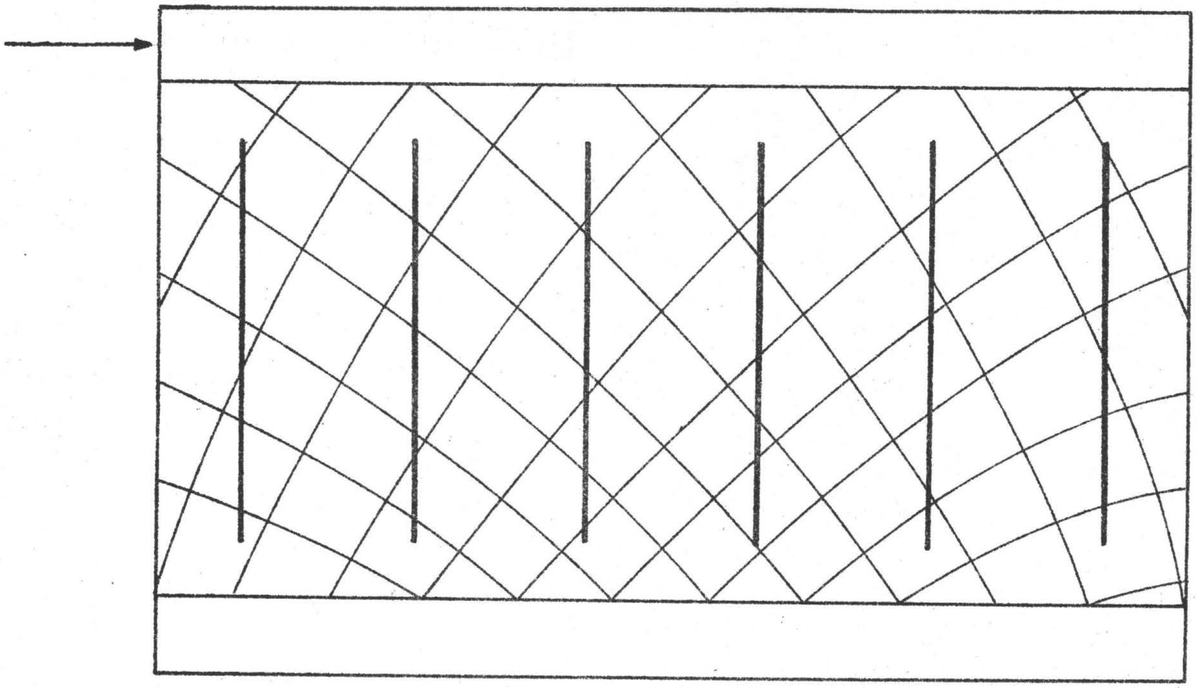

Fig. 21 PRINCIPAL STRESS TRAJECTORIES FOR PANELS A AND C

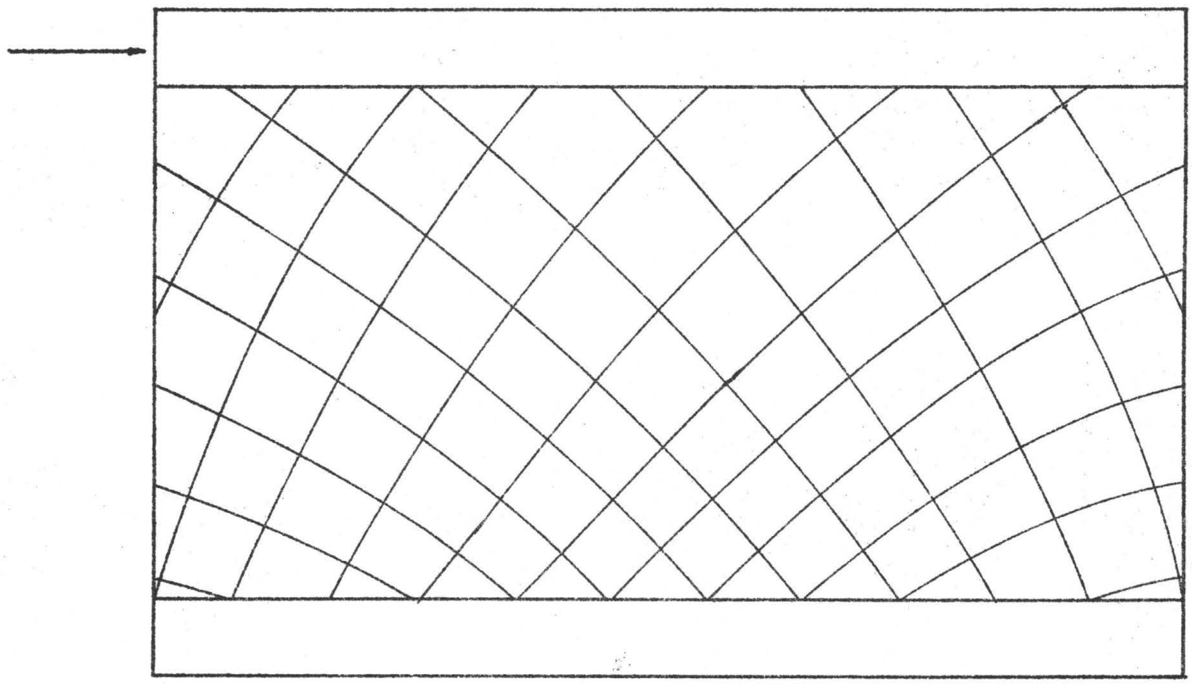

Fig. 22 PRINCIPAL STRESS TRAJECTORIES FOR PANEL B

the stress trajectories for panels A, B and C. Using this elastic theory cracks are considered to form when the intensity of the tensile principal stress reaches the tensile strength of the concrete. It is found, however, that the cracking load is much lower than that predicted by the principal stress theory and the tensile strength of concrete. This is due to the presence of shrinkage stresses and to local weakening of the cross section by transverse reinforcement.

5.3 Crack Formations of Panel A

For Panel A the position of formation of the initial cracks agrees with the principal stress trajectories. The first crack formed in the 4th cycle, under a lateral load of 38.5 kips and a lateral displacement of .16 in., at the left hand end interface between the wall and the lower flange beam. The corresponding tensile stress was calculated as 267 p.s.i. using the principal stress theory. In the same cycle, on the reversal of lateral load, a similar crack formed at the right hand end. The lateral load in this case was 35.7 kips and the lateral displacement was .13 in. while the corresponding tensile stress was 248 p.s.i. After the initial visible cracking the principal stress trajectories may be altered considerably. However, for Panel A the next cracking position can be reconciled with the original principal stress trajectories. These cracks originated at the ends of the vertical slits and propagated towards the flange beams. In many cases the cracks were inclined at angles very similar to the corresponding stress trajectories. In the forward cycle of lateral load these diagonal cracks occurred throughout the 5th cycle while in the reverse direction the cracks formed, with the flexural interface crack, at a lateral load of 35.7 kips. The flexural crack formed first followed by the series of short diagonal cracks. At this stage of the sequence of lateral load cycling the vertical slits became lines of weakness and as cracking in reinforced concrete members occurs at points of least resistance, the positions of the formation of cracks was influenced by the vertical slits.

The formation of the larger cracks in Panel A, appear as dramatic changes of slope on the load-deflection curves. Some of the more important cracks are referenced on Figures 24 and 32. Cracking usually occurred in the first cycle of the series of three at the same displacement. The only major exception was in the formation of the diagonal cracks in the forward cycle of lateral load. In this particular case the lateral load of the previous cycle had seriously weakened the concrete in the critical regions. The diagonal cracks, originating from the slits, formed at lateral loads ranging from 9.7 kips to 31.3 kips.

Essentially all the cracking in Panel A, occurred in the first seven cycles of lateral load. In the remaining cycles a well defined resistance mechanism formed. It consisted of diagonal cracks from the end of the slits to the flange beam - wall interface, the cracks along the interface and the vertical slits. Figure 23 shows this mechanism. Relative movement was observed along the slits and along the major cracks of the resistance mechanism during the last few cycles of lateral loading.

The cracks which formed the resistance mechanism gradually increased in width during the last few cycles of lateral load. The cracks of the mechanism that developed in the forward cycle of lateral load completely closed on reversal of lateral load. Similarly with the crack mechanism of the reverse cycle of lateral load. However, the major cracks of both mechanisms did not close when the load was removed. Load in the opposite direction was required to close them. In the final cycle the crack width of the major cracks was approximately 0.2 in., Figure 24 shows the final crack pattern of Panel A.

5.4 Crack Formations of Panel B

The first cracks in Panel B were flexural cracks and these formed at the interface between the lower flange beam and the wall. This position of initial cracking was the same as the position in Panel A and can be related directly to the stress trajectories of Figure 22. The left hand end flexural cracks occurred in the 4th cycle under a lateral load of 34.0 kips, a lateral deflection of .13 in., and corresponding tensile stress of 236 p.s.i.. While the right hand end flexural cracks formed in the same cycle under a reversed lateral load

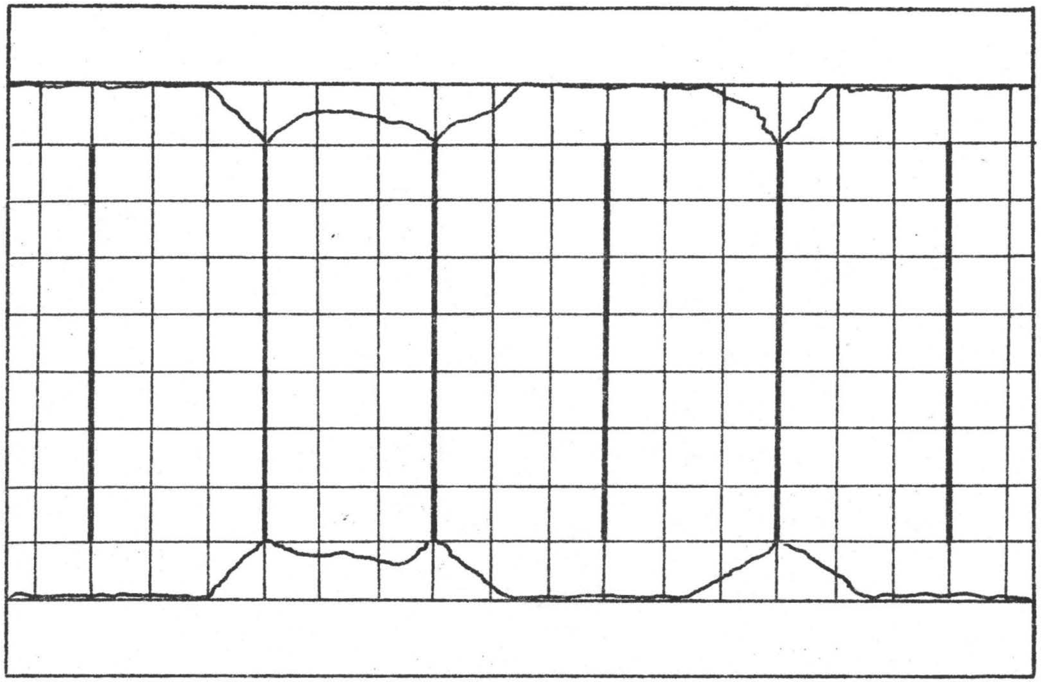

Fig. 23 RESISTANCE MECHANISM OF PANEL A

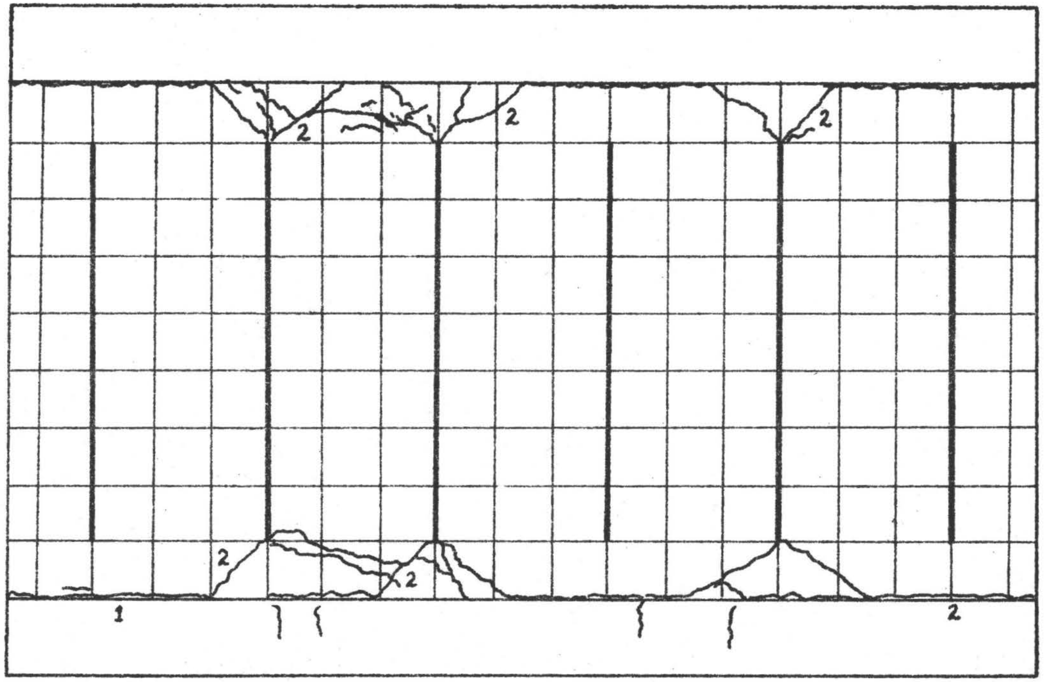

Numbers refer to position of crack formation shown on Fig. 32 Load-Deflection Relationship for Panel A

Fig. 24 FINAL CRACK PATTERN OF PANEL A

of 37.0 kip, a lateral deflection of .09 in., and a corresponding tensile stress of 257 p.s.i..

The second stage of cracking in Panel B can also be related to the stress trajectories. In the forward part of the 7th cycle at a lateral load of 42.1 kips and lateral displacement of .21 in. a crack started at the left hand end, 18 inches above the lower flange beam and propagated downwards at an angle of 63° to the vertical. The path of the crack follows the corresponding stress trajectory. In the same cycle, at a reversed lateral load of 45.4 kips and lateral displacement of .16 in., a similar crack formed at the right hand end. This crack started 15 inches above the lower flange beam and was inclined at an angle of 61° to the vertical. A corresponding line can be found on the stress trajectory diagram.

Further cracking in Panel B was limited to an additional diagonal crack at the left hand end, cracking along the lower flange beam - wall interface and a few cracks in the lower flange beam. The diagonal crack at the left hand end formed gradually in the 7th cycle. The crack started 10 inches above the lower flange beam and was inclined at an angle of 48° to the vertical. During the 7th cycle at a lateral load of 48.9 kips in the backwards portion of the lateral loading cycle, Panel B was completely cracked along the lower interface. Cracking in the lower flange beam occurred simultaneously with the formation of the flexural and diagonal cracks in the wall.

In the six remaining cycles of lateral load only two further small cracks formed. Both of these occurred in the lower flange beam. The resistance to the lateral load was offered by diagonal cracks at each end and by the crack along the lower interface. On the removal of load the crack mechanism would not close completely. Complete closure only occurred when lateral load in the reverse direction was applied. In the last few cycles at relative large lateral displacements (maximum in the 13th cycle was 0.67 in.) flexural crack widths as great as 0.2 in. were observed. Yielding of the vertical reinforcing bars in the regions of the flexural cracks was evident upon visual inspection after the completion of the thirteen lateral load cycles.

On the formation of the flexural cracks and the main diagonal cracks in wall panel B large slope changes occur on the load-deflection curves. The more important cracks are referenced in Figure 33. The formation of cracks occurred mainly in the first cycle of the series of three cycles at the same displacement. The final crack pattern of panel B is shown in Figure 25.

5.5 Crack Formations of Panel C

The formation of cracks in Panel C differed substantially from the cracking behaviour of the similar panel in test 1. The only difference between the two tests was the addition of the two vertical point loads in the third test

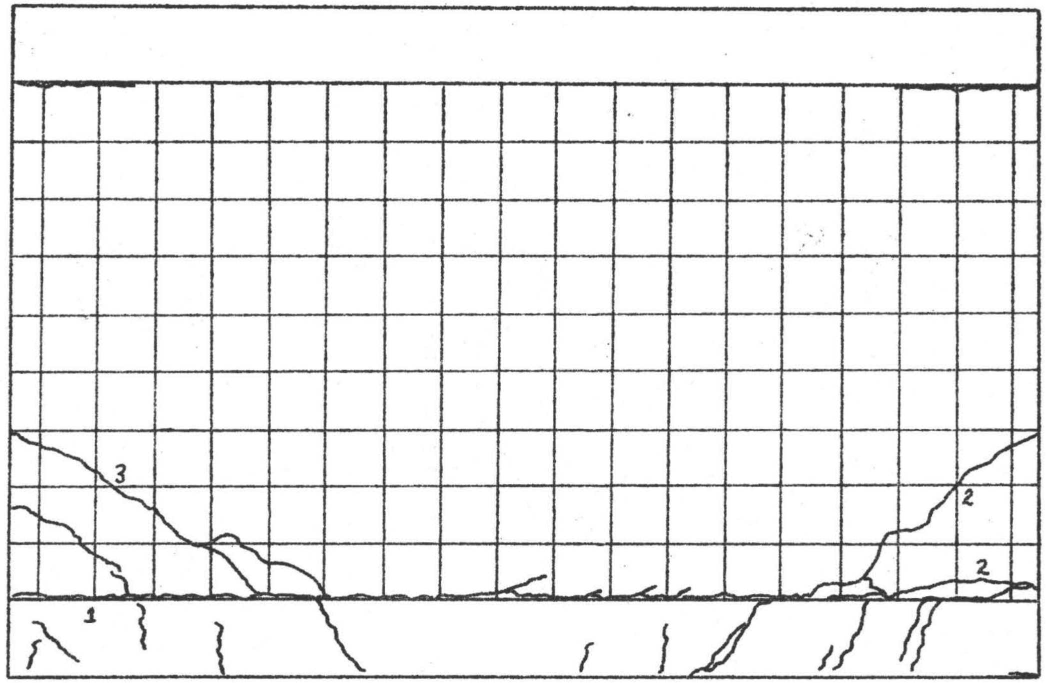

Numbers refer to position of crack formations shown on Fig. 33 Load-Deflection Relatio
ship for Panel B.

Fig. 25 FINAL CRACK PATTERN OF PANEL B

The different order of crack formation in panel C appears to be due entirely to the presence of the vertical loads.

The vertical loads were applied before the commencement of the lateral load cycling. Slight displacements in the vertical slits, directly below the load bear plates, were noticed on the application of the 75 kip point loads. No cracking was observed at this stage.

The initial visible cracks occurred in the forward portion of the first cycle at a lateral load of 33.2 kips and a lateral displacement of .05 in.. The position of the initial cracks can be directly related to the presence of the vertical loads. The diagonal cracks formed between the upper ends of the vertical slits and the points of application of the vertical loads. Also a 45° diagonal crack formed between the lower end of the third slit from the left hand end and the flange beam-wall interface. The corresponding cracks due to lateral load in the reverse direction did not occur until the 4th cycle. The lateral load at this point was 38.8 kips while the lateral deflection .07 in.. At the next incremental displacement point under a lateral load of 45.7 kips and lateral displacement of .08 in. further diagonal cracking occurred.

The direction of the initial diagonal cracks resembles in a general way the paths of the stress trajectories of Figure 21. In the derivation of the stress trajectories no account was taken of the effect of the properties of the asbestos sheet in the slits. Nor was any account taken of the effect on the stress trajectories, of the two vertical point loads. Consequently the stress trajectories of Figure 21 can only be used as a rough guide in assessing the direction of cracks. It is doubtful, even if these two factors could be included, whether an accurate prediction of cracking could be made using this technique. There is no means of including the initial movement of the vertical slits, due to the application of the vertical loads, which greatly influenced the pattern of crack formation.

Unlike the previous two tests, cracking was not confined to the first cycle of the series of three cycles at the same displacement. However the major cracking occurred in the first cycle and only the less significant cracks formed in the remaining two cycles.

The formation of cracks in Panel C was fairly evenly distributed throughout the final ten cycles. As previously noted only one set of visible cracks occurred in the first three cycles. In many cases very small, fine cracks formed which could not be detected as a change of slope on the lateral load-deflection diagram. Generally the changes in slope on the load-deflection curves, brought about by cracking, was less severe than in the previous two tests. There are only a couple of instances where long crack formations brought about significant changes. These are referenced on Figure 26 and 34.

Cracking along the lower flange beam-wall interface was not nearly as well developed in panel C as in panel A of test 1. At the left-hand end the flexural crack did not occur until the 7th cycle under a lateral load of 49.7 kips. The lateral displacement at this point along the line of application of the lateral load was 0.13 inches. At the right hand end a flexural crack did not occur at the lower flange beam-wall interface. A flexural crack was formed, however, in the 5th cycle at a lateral load of 23.5 kips and corresponding lateral displacement of 0.05 inches, 17 inches above the lower flange beam. This crack gradually lengthened in the remaining lateral load cycles.

A crack did form at the right hand end lower flange beam-wall interface. This crack formed in the final cycle at a lateral load of 87.0 kips and displacement of .47 inches. This was a diagonal crack and it originated from the lower end of the right hand end slit.

The final crack pattern of Panel C is shown in Figure 26. The most significant features are the extensive cracking and the large number of these cracks which can be classified as diagonal cracks.

5.6 Crack Formation of Panel D

The long vertical slits of Panel D considerably affected the formation of cracks and the final crack pattern. Cracking occurred initially during the application of the two vertical point loads of 75 kips which was carried out before the first

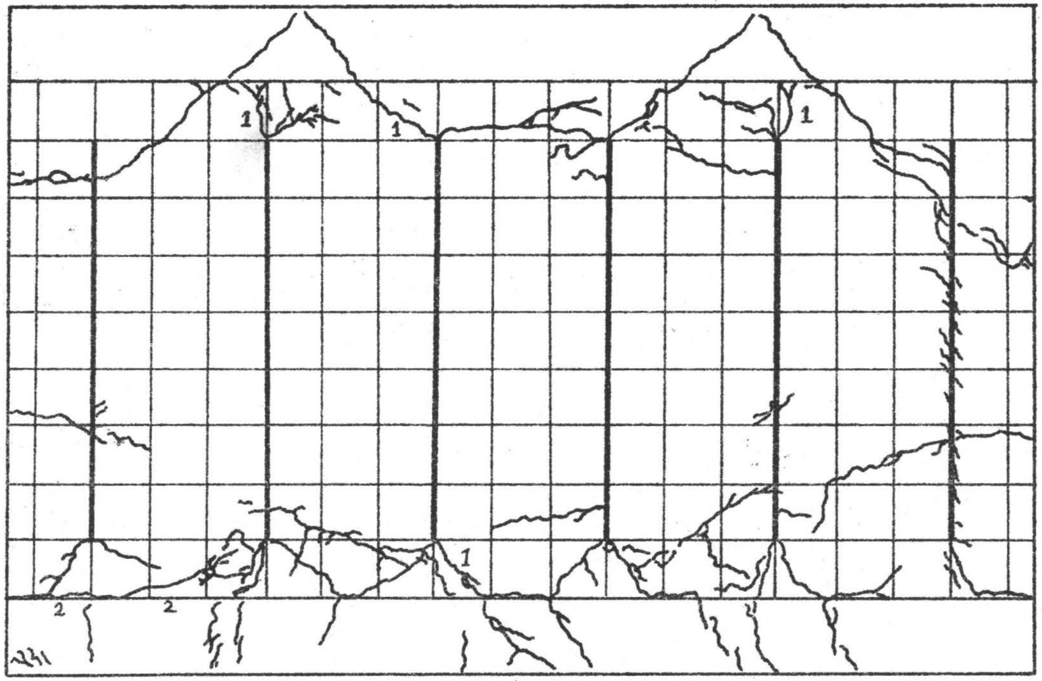

Numbers refer to position of crack formation shown on Fig. 34 Load-Deflection Relationship for Panel C.

Fig. 26 FINAL CRACK PATTERN OF PANEL C

lateral loading cycle. Movement of the vertical slits directly below the load bearing plates was observed during this process. The cracking caused by the application of the vertical loads was slight and consisted mainly of a crack in the upper flange beam between the vertical slits and the vertical load bearing plates.

The first cracks to appear under the lateral load cycling were located in the lower flange beam. No records of the crack formation in the upper flange beam was possible as the steel plates of the loading yoke completely covered the sides of the beam. However it was possible to note the formation of cracks in this flange beam on application of the vertical loads as these cracks were visible on the underside of the flange beam. The first cracks in the lower flange beam occurred at a lateral load of 42.3 kips during the first cycle. It is apparent that the inclusion of the panel-high vertical slits allowed the wall to deflect laterally without the panel section cracking. Initially the wall and the flange beams deflected as a single unit and short diagonal cracks formed in the relatively stiff lower flange beam. These diagonal cracks commenced at the interface and propagated into the flange beam.

Flexural cracking at the left hand end flange beam-wall interface did not occur until the 7th cycle at a lateral load of 45.90 kips and corresponding lateral displacement of 0.16 in. The formation of this crack is characterized by a sudden change in the slope of the load-deflection curve. It is interesting to note that the corresponding flexural crack did not form at the right hand end. Cracking at this position was due to the continuation of a small diagonal crack which originated from the vertical slits. This crack occurred in the 10th cycle at a lateral load of 61.3 kips and corresponding lateral deflection of 0.32 inches. Undoubtedly the concrete in this region had been cracked internally under tensile stresses but the visible cracking occurred in the manner described.

The formation of cracks in panel D was spread throughout the thirteen cycles of lateral load. Generally cracking caused only a modest change in the slope of the load deflection curve. The two major changes are referenced in Figure 27 and 35. In the final cycle, due to extensive cracking, the slope of the load-deflection diagram flattens out.

The final crack pattern of panel D is shown in Figure 27. The cracks are mainly located in the flange beams and at the shear wall-flange beam interface.

5.7 Summary

The main differences in the formation of the cracks in the four wall panels are directly related to the inclusion of the vertical slits and to the presence of the two vertical point loads. The vertical slits act as lines of weakness in the wall panels and thereby induce a particular pattern of cracks. The panel-high slits permit sufficient deformations

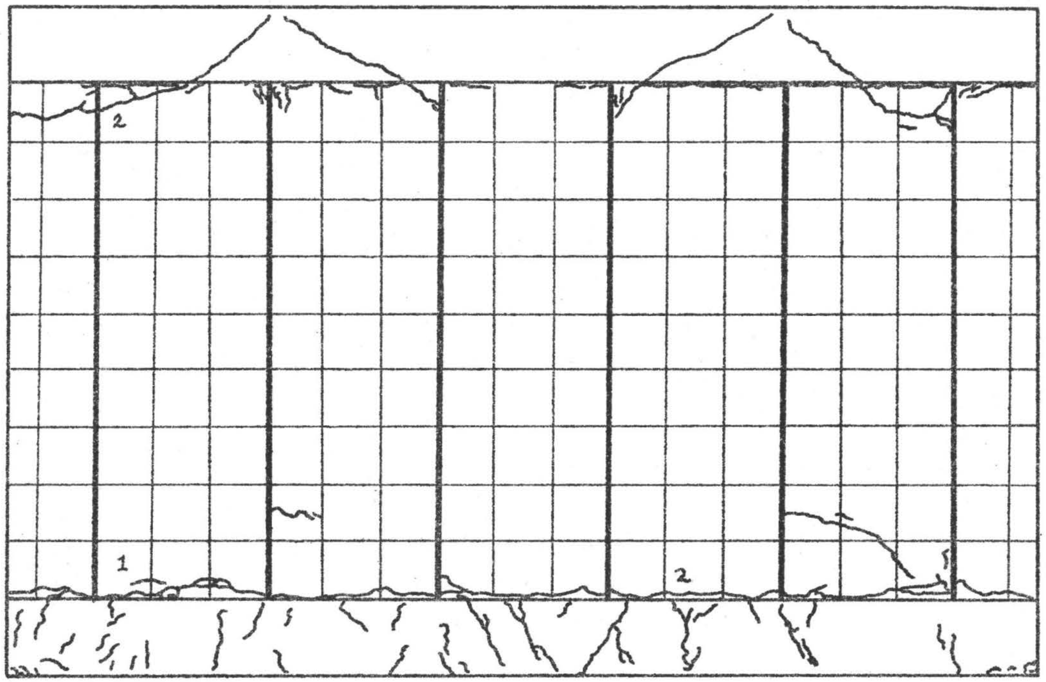

Numbers refer to position of crack formations shown on Fig. 35 Load-Deflection Relationships for Panel D.

Fig. 27 FINAL CRACK PATTERN OF PANEL D

in the wall to occur to prevent extensive cracking in the panel section.

The presence of the two vertical point loads altered the type of cracks formed. In the first two tests mostly flexural cracking occurred while in the final two diagonal cracking was more common. The width of the flexural cracks of the first two tests was greater while cracking in the final two tests was more extensive and the formation of cracks was more evenly distributed throughout the entire sequence of lateral displacements.

In order to assess the effect of the vertical loading system on the lateral response of the wall, the various movements of the vertical loading systems were monitored during the lateral loading cycles of Panels C and D. The changes in vertical load due to the movement of the wall were recorded. The range of the load change was ± 1 kip and it was concluded that the vertical loading appartus did not offer any effective restraint against lateral response.

The presence of the two vertical point loads in test 3 and 4 caused suppression of flexural cracking. Flexural cracking could not occur until the tensile stress in the wall panel was equal to the compressive stress induced by the vertical loads and the tensile strength of the concrete. Cracking prior to the formation of the flexural crack was caused by the combined action of the vertical slits and the point loads under lateral displacement. The vertical slits permitted enough deformation under lateral load for the diagonal cracks to form at the upper part of the panel between the point of application of the loads and the ends of the slits. In the lower half the diagonal cracks formed between the flange beam-wall interface and the ends of the slits.

CHAPTER VI

THE DEFLECTED SHAPES AND THE LOAD-DEFLECTION RELATIONSHIPS OF THE WALL PANELS

6.1 Deflected Shapes

A comparison of the recorded deflected shapes of each wall panel in the first cycle of the sequence of lateral loading is made with the deflected shapes obtained from theoretical considerations. The theoretical calculations consider a wall panel to be a perfectly elastic, homogeneous, isotropic contilever beam subjected to a point load applied at the end of the beam. The deflection of various points is computed using the modulus of elasticity determined from the concrete cylinder tests and a gross second moment of area of the wall section. Both shear and flexural effects are considered in the calculations of the deflected shapes.

$$\text{Deflection } y = \underbrace{\frac{Px^2}{6EI}(3\ell - x)}_{\text{Flexural}} + \underbrace{\frac{3Px}{AE}}_{\text{Shear}}$$

$$= \frac{3Px}{AE}\left[\frac{x(3\ell - x)A}{18I} + 1\right]$$

where

A = Area of concrete wall.

E = Elastic modulus of concrete.

I = Second moment of area of wall panel.

The theoretically calculated deflected shapes of the end walls and the experimentally recorded displacement points are shown on Figures 28, 29, 30 and 31. The recorded points follow in a general way, the calculated deflected shapes. The agreement is reasonably good at low deflection but at the larger displacements the discrepancy between the recorded and theoretical values increases. Two possible causes for this discrepancy can be identified but the extent of their contributions cannot be ascertained from the limited number of tests of this investigation.

In the first place a rotation of the base beam may affect the value of the recorded points. A base rotation correction, which assumed that the base beam remained perfectly rigid between the two deflection monitoring points, was carried out on the recorded displacements. In future tests the rotation of the base of the wall should be carefully controlled and if possible entirely eliminated.

Secondly the assumption made in the theoretical calculations that concrete is an elastic, homogeneous, isotropic material may not be correct. Concrete is known to begin its inelastic behaviour almost immediately on application of

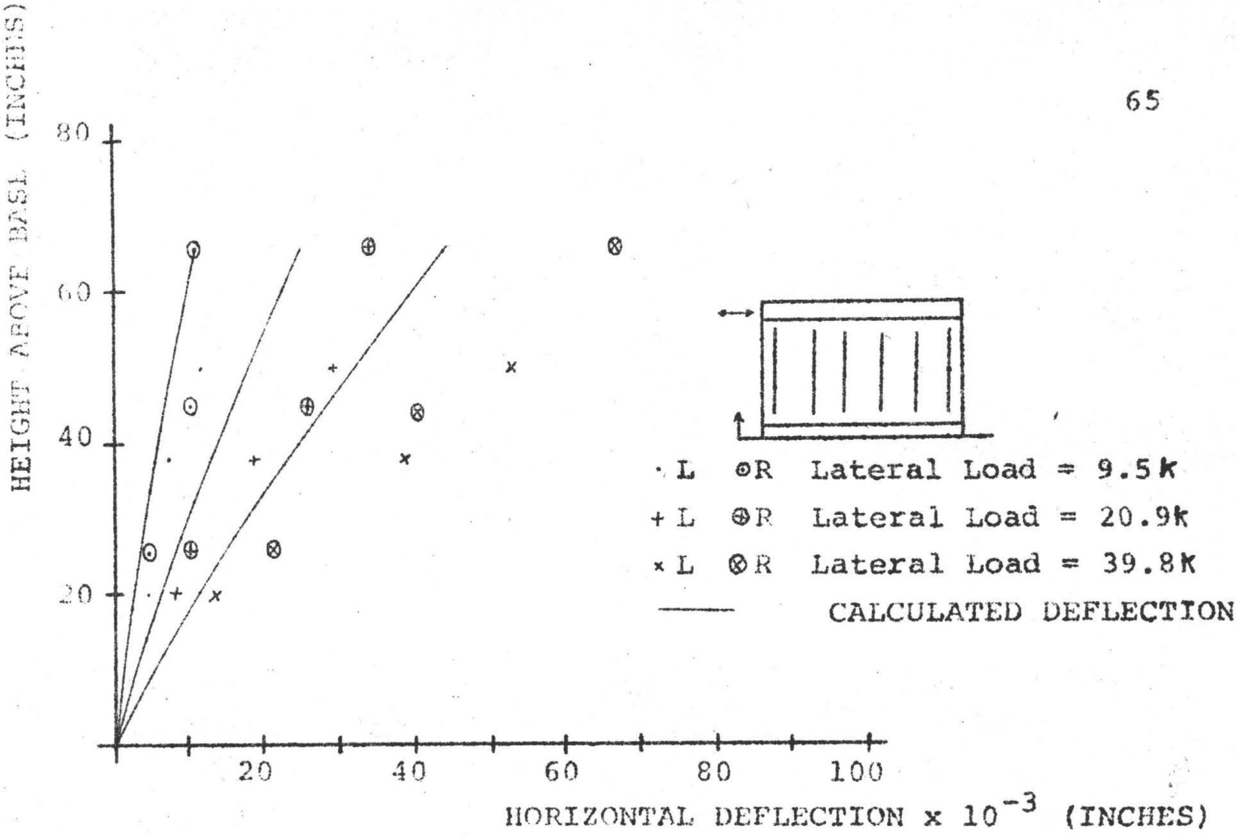

Fig. 28 LATERAL DEFLECTION OF PANEL A DURING FIRST CYCLE

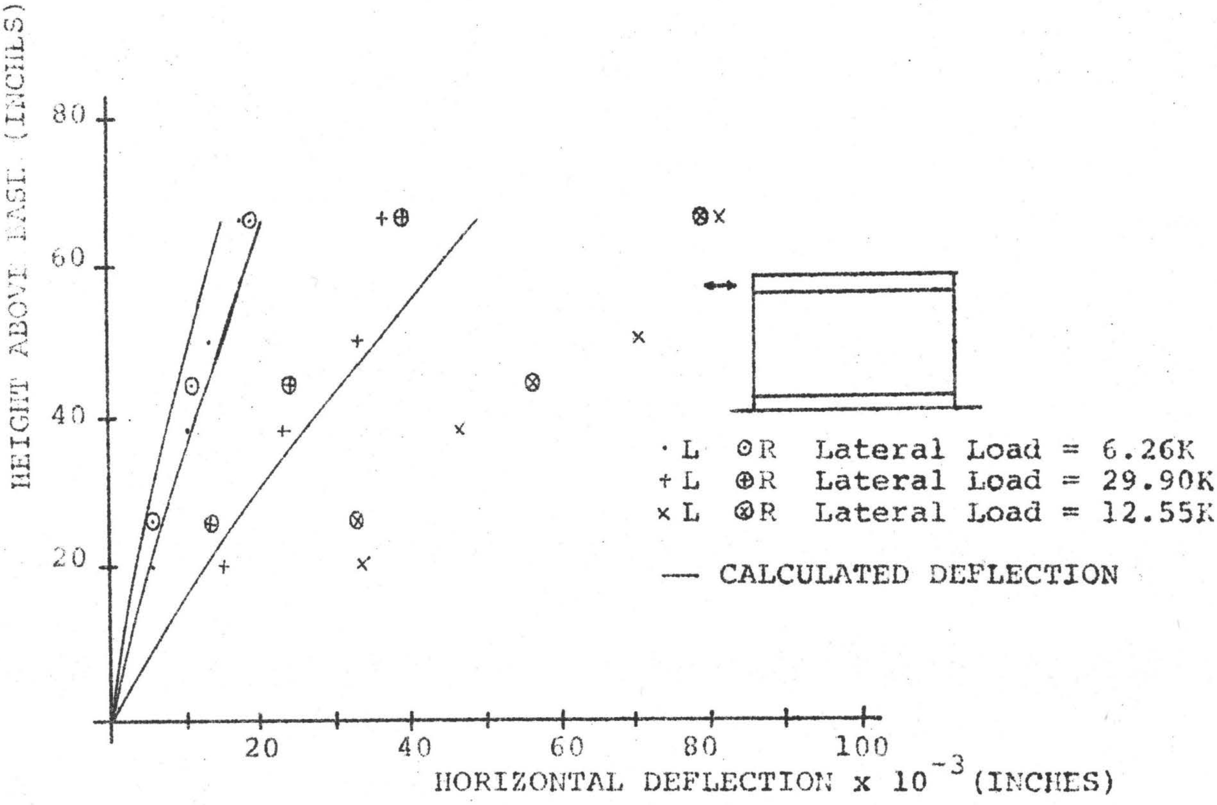

Fig. 29 LATERAL DEFLECTIONS OF PANEL B DURING FIRST CYCLE

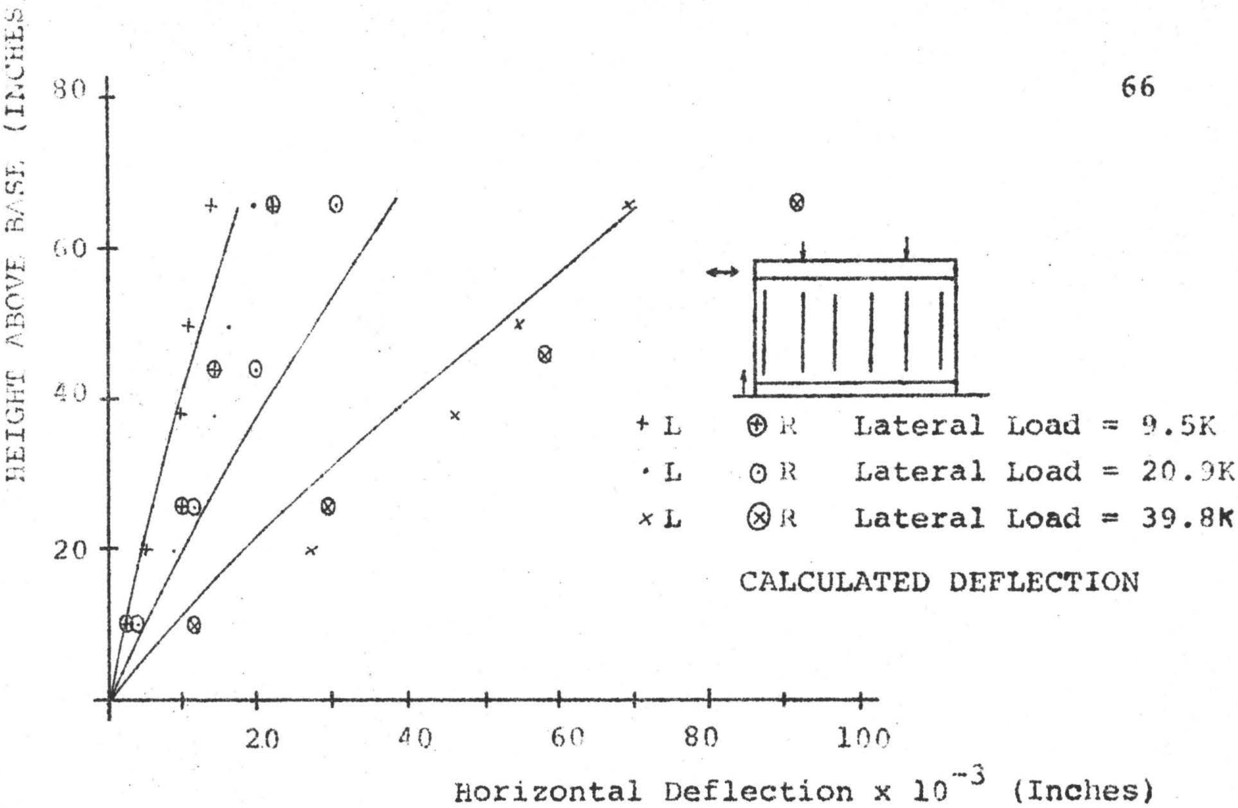

Fig. 30 LATERAL DEFLECTIONS OF PANEL C DURING FIRST CYCLE

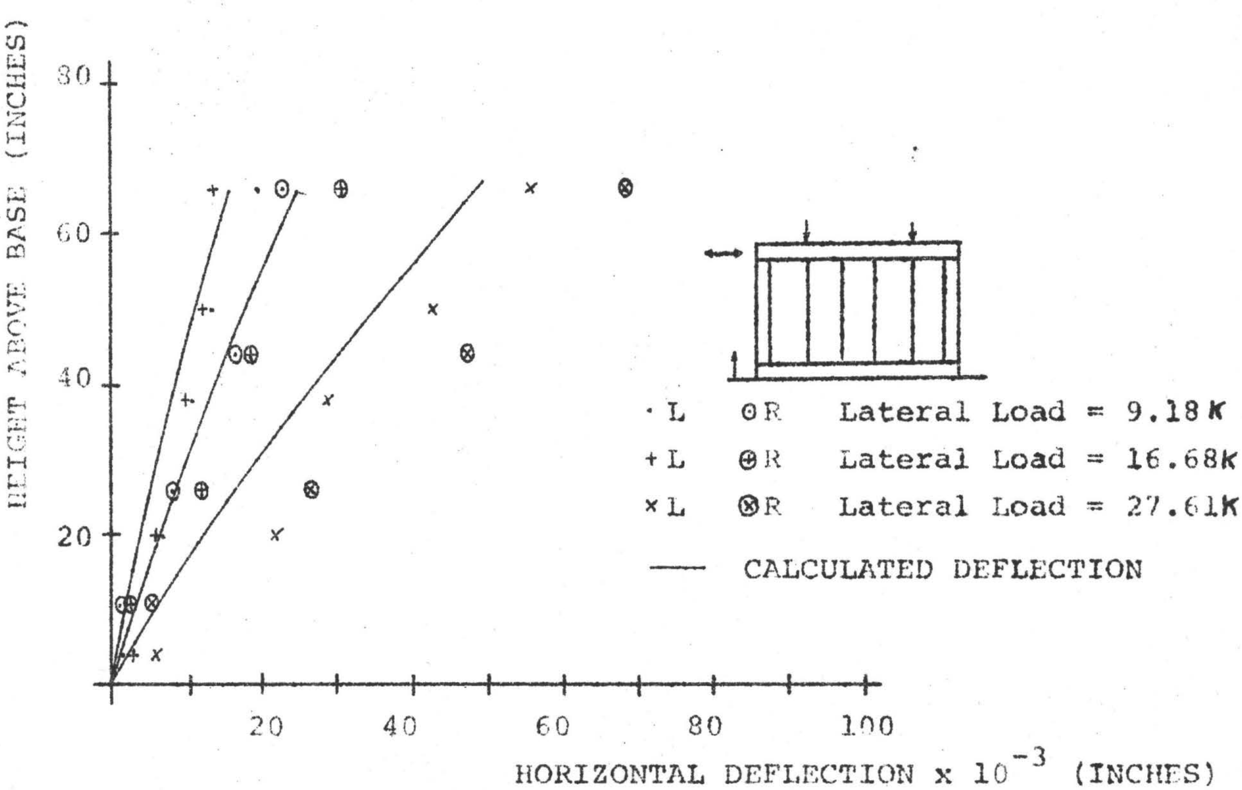

Fig. 31 LATERAL DEFLECTIONS OF PANEL D DURING FIRST CYCLE

loads. The inelastic behaviour of concrete and the deep beam effect may necessitate a completely new approach to deflection calculation of wall panels.

If reasonably realistic results are to be obtained from analysis of the response of shear wall buildings in the inelastic range a method is urgently required for the calculation of the stiffness of cracked elements. Paulay has suggested a method of determining the deflection of cracked shear wall coupling beams[21] and a similar approach would be valuable for cracked shear wall panels.

6.2 The Load-Deflection Relationships

6.2.1 Introduction

A great deal of relevant information can be obtained from the load-deflection diagrams of the four wall panels tested in this investigation. Information concerning the stiffness of the panels and the amount of energy dissipated during a lateral loading cycle is shown in these diagrams. A study of the set of load-deflection curves from each test reveals how the various properties of the shear wall panel were affected by the cycling of lateral loads.

6.2.2 Load-Deflection Diagrams

For each test, the first cycles of the various displacement positions are combined to form a continuous load deflection curve. The initial cycle commences at the origin and the rest start where the preceeding cycle ends. These curves (see Figures 32, 33, 34 and 35) do not represent the exact behaviour of the wall panels under the lateral cycling system used in this experimental investigation. The load-deflection curves of the second and third cycles of the series of three at the same displacement are similar in form to the first cycle. There is a slight decrease in the maximum lateral load and a decrease in the slope of the load-deflection curve. A load-deflection diagram containing all thirteen curves would be extremely difficut to interpret. Sufficient accuracy is obtained by including only 5 curves. The general trends of the load-deflection diagrams can be readily noted:

1. No decrease of load is experienced with increase in deflection.
2. The stiffness of the wall panels decrease with increase in deflection.
3. The amount of energy dissipated in a cycle increases with increase in deflection.

A detailed description of stiffness and energy considerations is given in separate sections.

6.2.3 Load Carrying Capacity of The Wall Panels

The load deflection diagrams show the effect of the vertical loads on the lateral load carrying capabilities of the wall panels. A large increase in the lateral load values occurred in tests three and four. Panel C has

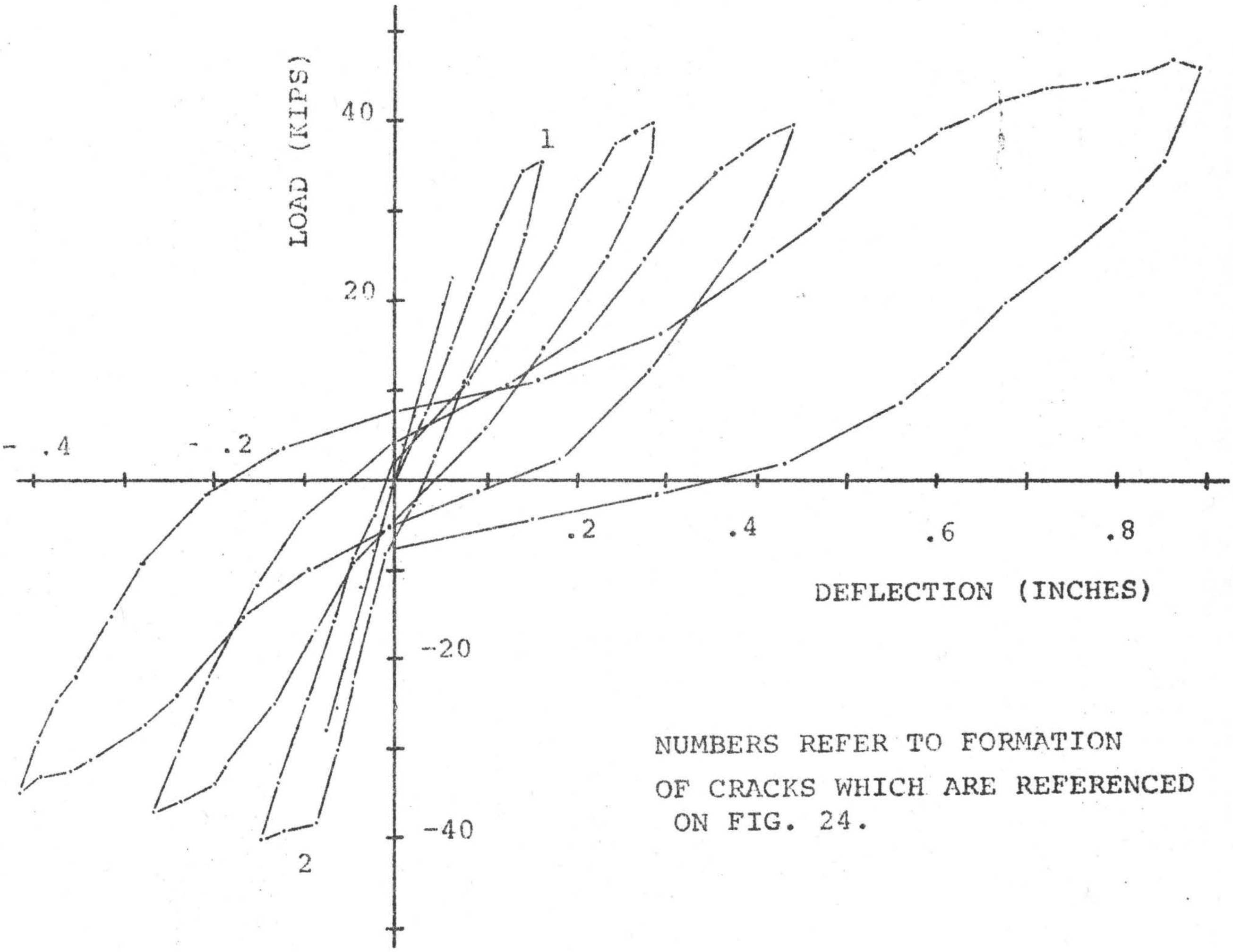

Fig. 32 THE LOAD-DEFLECTION RELATIONSHIP FOR PANEL A

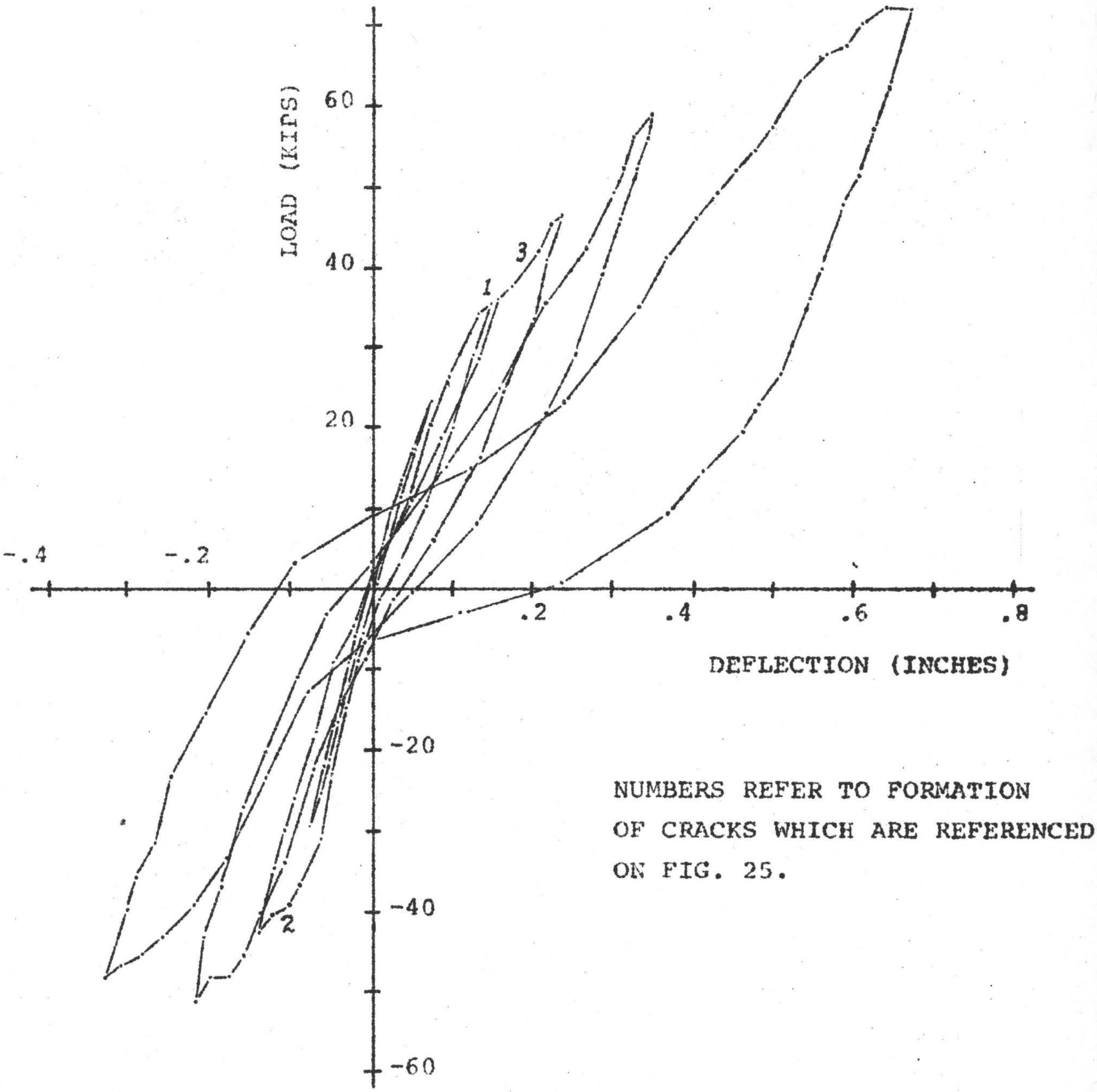

Fig. 33 THE LOAD-DEFLECTION RELATIONSHIP FOR PANEL B

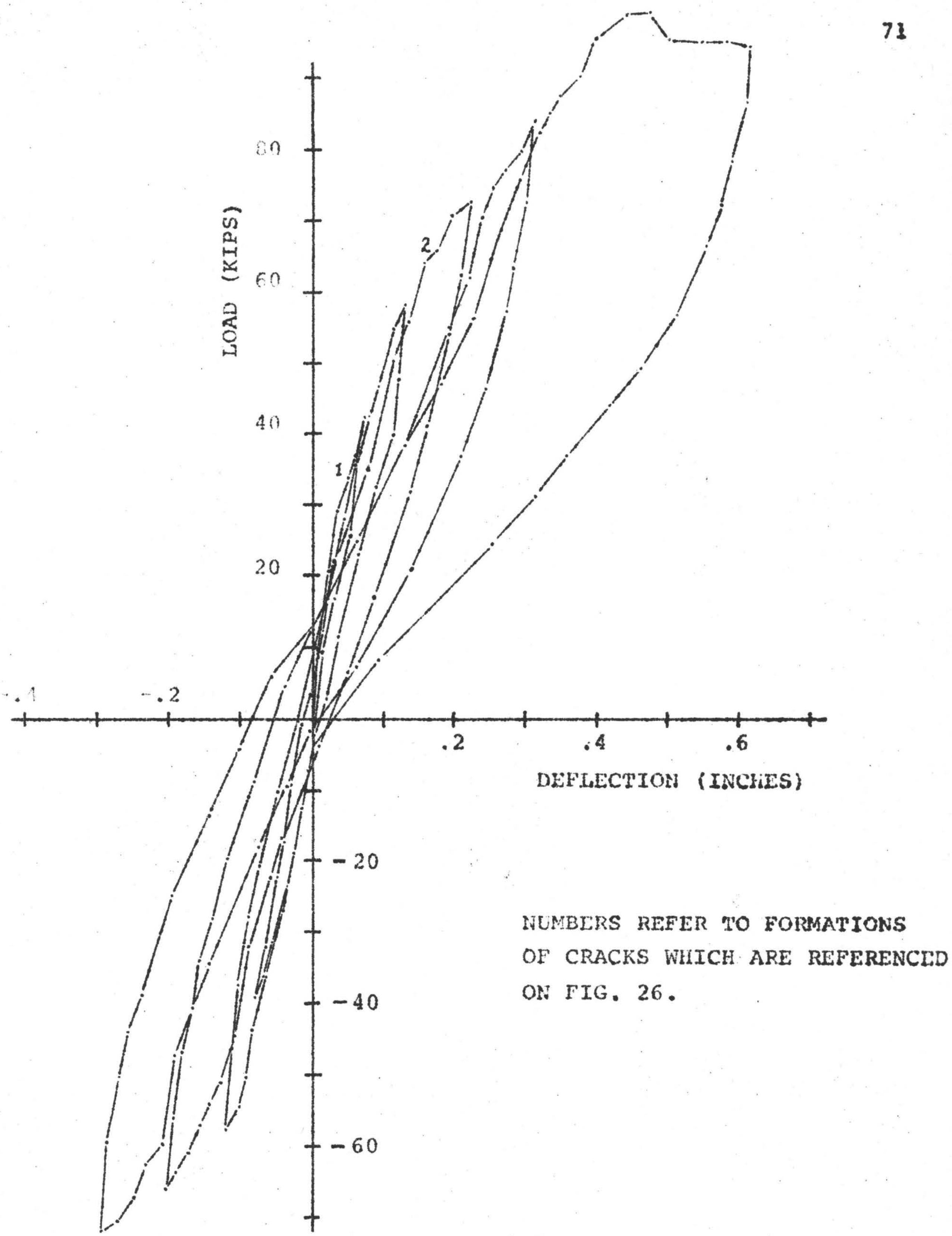

Fig. 34 THE LOAD-DEFLECTION RELATIONSHIP FOR PANEL C

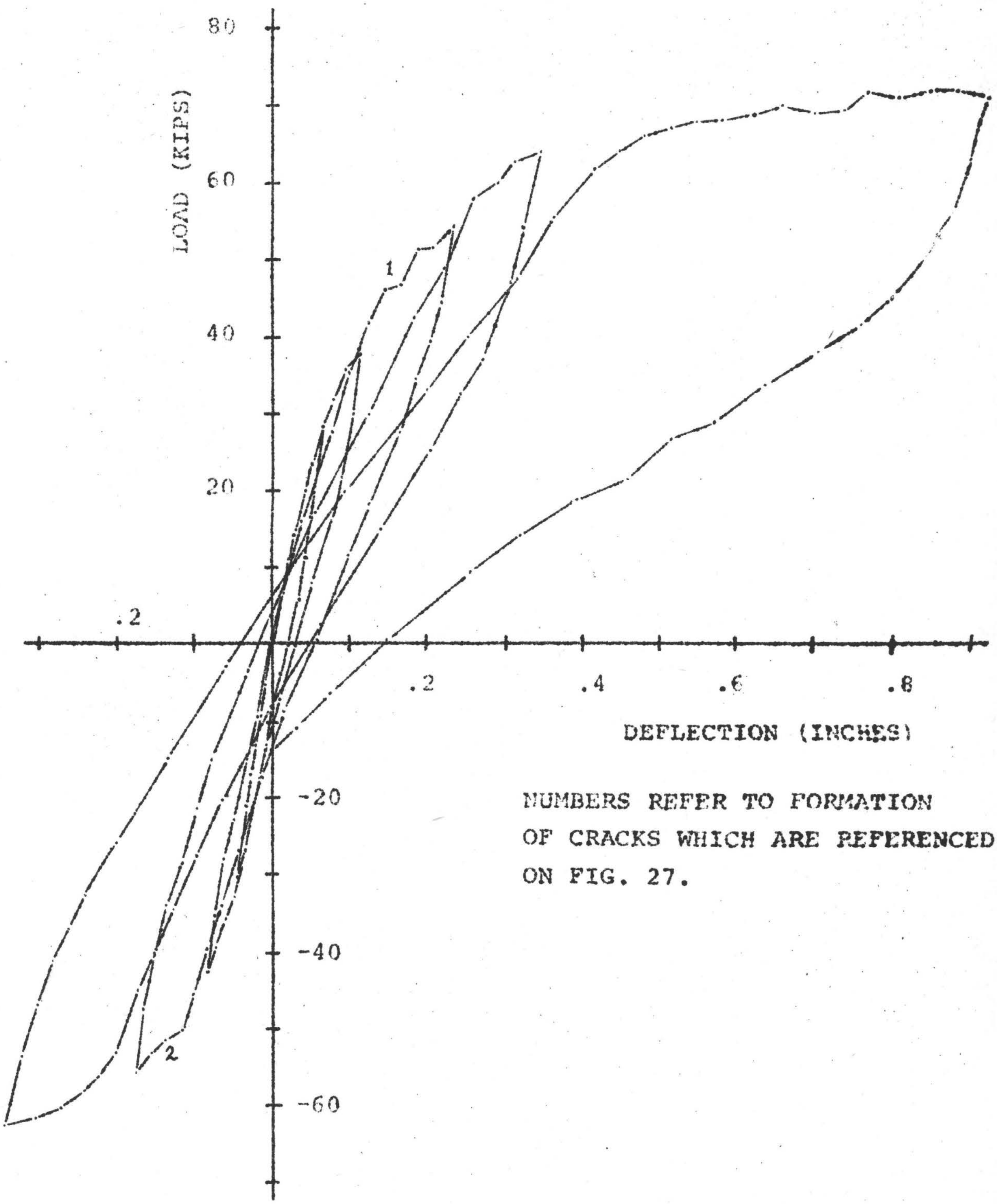

Fig. 35 THE LOAD-DEFLECTION RELATIONSHIP FOR PANEL D

approximately twice the lateral load carrying capacity of Panel A.

The vertical loads apply a compressive stress to the concrete wall section. This condition suppresses the formation of flexural cracks until the lateral force is sufficient to induce tensile stresses equal to the initial compressive stresses and the tensile strength of the concrete. In the section on crack formation it was pointed out that for panel C the flexural crack in the forward cycle occurred at a lateral load of 47.9 kips, while the corresponding crack in panel A occurred at a lateral load of 38.5 kips. In the reverse direction the flexural crack at the flange beam-wall interface occurred at a lateral load of 35.7 kips for panel A but a corresponding crack did not occur in panel C. A diagonal crack did form in panel C 17 in. above the lower interface at a lateral load of 23.5 kips.

Diagonal cracking occurred in panel C prior to the formation of the flexural cracks. The diagonal cracks which are located between the end of the slits and the flange beam wall interface affected the response of the wall panel to lateral load. The width of the diagonal cracks was small and transfer of shear along the crack was possible by aggregate interlock forces and the dowel forces of the reinforcing steel. In panel A the crack widths of the resistance mechanism were large and only the dowel forces of the reinforcing steel acted in the transfer of shear along the cracks. A study of the mechanics of shear resistance in concrete beams[33] showed that the aggregate interlock forces are approximately three times as great as the dowel forces of the reinforcing steel. Hence the large increase in strength of panel C.

6.2.4 Backbone Curves

A load-deflection diagram for each test was drawn using average values of the load and deflection for the 3 successive cycles of the displacement points. The resulting curves are known as "backbone" curves[35]. These curves give an overall picture of the energy absorbed by the various wall panels. It is important to note that many features of the inelastic action of reinforced concrete walls are not displayed on these diagrams. No indication is given from these diagrams of the ability of the concrete walls to dissipate energy through inelastic action. Many erroneous conclusions have been drawn from similar diagrams of prestressed concrete members on the ability of this material to withstand seismic ground motions[36]. In addition no information is given on how the stiffness of the wall is affected by cycling lateral load.

The backbone curves for the wall panel indicate an elasto-plastic material. The load-deflection diagrams constructed from the recorded data show that this is definitely not the case. However the backbone curves do show that the load does not fall off as the lateral displacement is increased.

The ductility factors calculated from these diagrams show that the wall panels possess sufficient inelastic deflection capabilities for normal practical purposes.

6.2.5 Reduction Factors

The backbone curve could provide information on the energy dissipation capabilities of the shear wall panels if the amount of energy absorbed is equated to the load and deflection in the following manner.

Energy dissipated = $f \times P \times D$

f = energy reduction factor

P = lateral load

D = lateral displacement

Only energy absorbed after cracking is considered by this equation as the energy absorbed by elastic action is small and can safely be ignored.

A plot of energy reduction factor vs deflection is shown in Figure 37. It is further assumed that the reduction factors is a function of the lateral deflection.

$$f = \mathit{f}(D)$$

The plotted points for panel C in Figure 37, for example, appear to follow the general pattern of a parabola about the x-axis. It is, therefore, assumed that the energy reduction factor equation can be written as

$$f = K \times D^{1/2}$$

K = constant

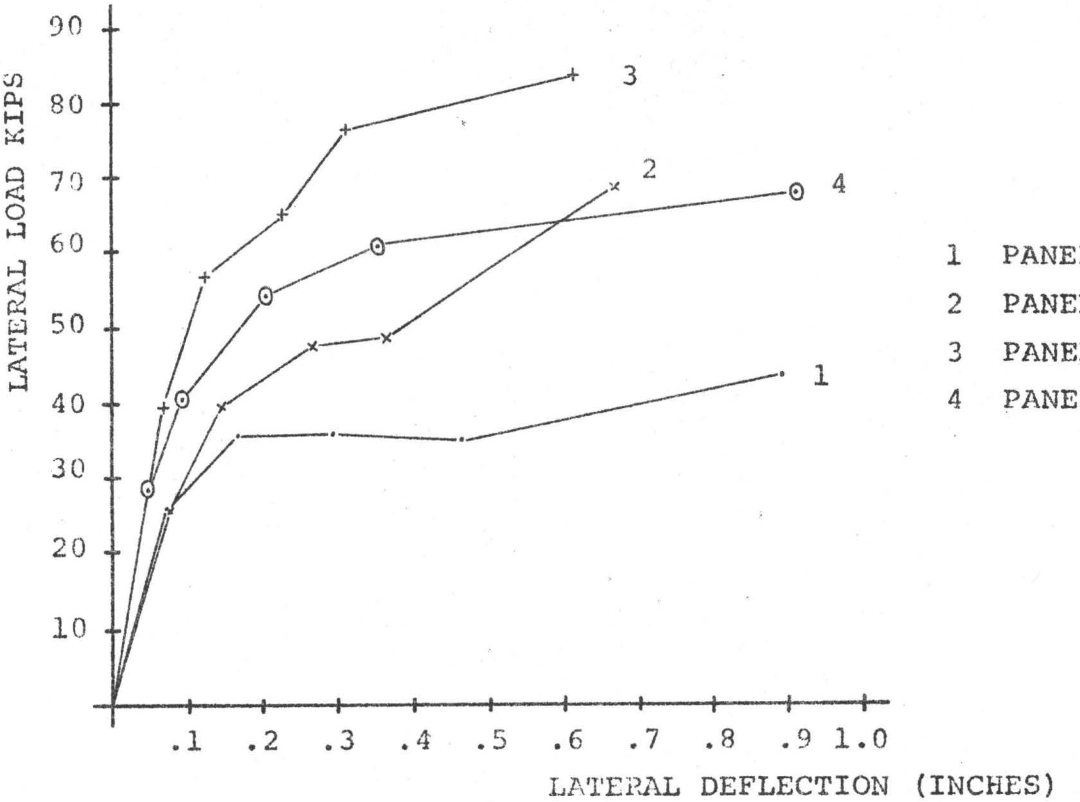

FIG. 36 BACKBONE CURVES

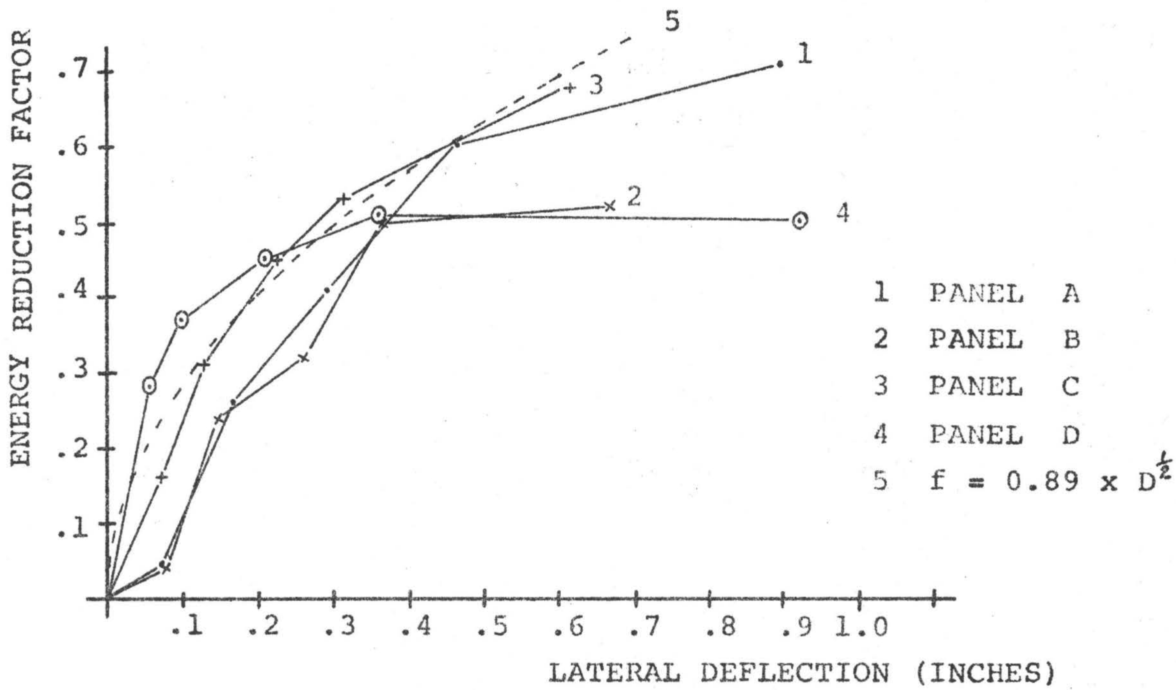

FIG. 37 ENERGY REDUCTION FACTOR - LATERAL DEFLECTION RELATIONSHIP

For panel C the value of the constant was found at points $D = .5$ and $f = .63$ The equation of the energy reduction factor curve becomes

$$f = 0.89 \times D^{1/2}$$

A reasonably good correlation results. Similar expressions for the other panels can be found. It should be noted that the reduction factor curves of panels A and C follow the same general shape. These panels were identical in structural details and differed only in the system of loading.

The sequence of lateral loading cycles of this investigation differed from the loading cycles normally used in studies to determine backbone curves[37]. Generally backbone curves are constructed from tests which increase the deflection and load after each cycle. However a study of an earthquake ground motion record will reveal that the displacements bear no resemblance to the gradually increasing load and deflection cycles. This type of approach does not consider the possibility of several cycles occurring at the same displacement. In the 4 tests of this investigation this possibility was incorporated into the cycling sequence. At each displacement position the reduction factor was calculated using the energy dissipation value of only the first cycle. The energy dissipation values of the other two cycles are considered as an energy reserve for possible cycling at the same or lesser displacements.

CHAPTER VII

THE STIFFNESS AND ENERGY PROPERTIES OF THE WALL PANELS

7.1 Stiffness

7.1.1 Introduction

In an analytical investigation of the response of a structure to a severe earthquake the stiffness of the various structural components must be known. The effect of inelastic excursions on the stiffness of these components should be incorporated in such an analysis to establish the true response behaviour of the structure.

7.1.2 Stiffness Degradation

A significant deterioration in the stiffness of the wall panels occurred under repeated cyclic lateral loading in the inelastic range. The total amount of stiffness deterioration was approximately 80 per cent of the initial stiffness for panels A and B and approximately 75 per cent for panels C and D. Similar results for reinforced concrete members subjected to repeated lateral cyclic loading have been reported in the literature[21,38,39].

The effect of repeated lateral load cycling on the stiffness of the wall panels is displayed in the load-deflection diagrams of Figures 32, 33, 34, and 35. The deterioration in stiffness starts on the curves at the point corresponding to initial cracking and continues throughout the remaining cycles.

Cracking is the primary process of stiffness degradation while three other processes; inelastic behaviour of the reinforcing steel, deterioration of bond, and shear displacements along the cracks, are related to the cracking behaviour.

7.1.2.1 Effect of Cracking

Cracks affect the stiffness in several ways. On the formation of cracks there is a sudden change of slope in the load deflection relationship and the amount of change depends on the extent of the new cracking. In panels A and B large flexural cracks formed in the fourth cycle of the sequential lateral loading pattern and the corresponding changes of slopes are displayed on the load deflection curves of Figures 32 and 33. Similar slope changes occur in the load-deflection diagrams of panels C and D, (Figures 34 and 35), due to the formation of the large diagonal cracks.

In the lateral loading cycles after initial cracking, the only resistance to load in the region of the cracks is provided by the reinforcing steel. The amount of stiffness reduction depends on the bond forces between the concrete and reinforcing steel and on the properties of the reinforcing steel.

On removal of the lateral load the cracks do not close and a significant reduction in stiffness occurs. The compressive forces across the cracks are initially transferred by the reinforcing steel. An increase in the stiffness occurs when the cracks close and the compression forces are transferred by the bearing of the two concrete surfaces.

The effects of the cracking process on the determination of stiffness explains the occurrence of the three distinct stiffness zones in the second half of the sequence of lateral loading cycles.

(I) Initial Zone: The stiffness in this region is low. Lateral load is required to close the cracks formed during loading in the opposite direction. Until the cracks have closed the compression forces are transferred across the cracks by the reinforcing steel.

(II) Middle Zone: The cracks have now closed and this results in an increase of slope on the load-deflection curve. The compression forces are transferred across the cracks by the bearing of the two concrete surfaces.

(III) Final Zone: In this zone further cracking of the concrete and yielding of the reinforcing steel causes a decrease in the slope of the load-deflection curves.

The extent of the development of the first two zones depends on the width of the cracks formed under lateral load from the reverse direction. In panels A and B, the tests involving only lateral load, relatively large crack widths occurred and all three zones are clearly identifiable in Figures 32 and 33. In comparison, the crack widths of panels C and D were smaller and the three zones are harder to distinguish in Figures 34 and 35.

7.1.2.2 The Effects of the Inelastic Behaviour of the Reinforcing Steel

In the previous section the role of the reinforcing steel in the transfer of forces across the cracks was explained. The effect of this process on the overall stiffness depends on the properties of the reinforcing steel. If the steel exhibits a pronounced Bauschinger effect a large stiffness reduction will occur. Unfortunately a sample of the panel reinforcing had insufficient cross sectional area to enable this effect to be investigated. Consequently no firm conclusions can be made on the effect of this phenomenon on the stiffness degradation. Repeated load tests carried out on reinforced concrete beams have illustrated the dependence of the load-deflection relationship on the Bauschinger effect[25,39].

7.1.2.3 The Effect of Bond

A deterioration of the stress transfer between concrete and the reinforcing steel produces a widening of cracks and thereby causes a reduction in the stiffness. The bond deterioration of the reinforcing steel in the wall panels of this investigation would be greater than that experienced by full size wall panels under similar conditions. Deformed bars would be used in full size walls, in place of the smooth bars of the half scale models.

The stress transfer between concrete and reinforcing steel is achieved by:[40]

1. Chemical adhesion

2. Friction

3. Mechanical interaction between concrete and steel.

Smooth round bars depend primarily on chemical adhesive and friction for bond while some mechanical interaction occurs due to the roughness of the steel bars. Once the chemical adhesion has been broken, friction and the small mechanical interaction are the only means of resisting the bond forces. In comparison deformed bars depend mainly on the mechanical interlocking for their superior bond properties. Therefore the stiffness degradation due to bond determinatinn would be greatly improved by the use of deformed bars.

7.1.2.4 The Effect of Shear Deformation Along the Cracks

The presence of shear forces on the region of cracks tends to cause a relative displacement of the crack's two surfaces. This tendency is resisted by the interlocking forces of the aggregate particles in the surfaces of the crack and by the dowel forces of the reinforcing steel. The reinforcing steel is pressed against the concrete and high local stresses are induced which causes a deterioration in the bond resistance. For large open cracks only the dowel forces in the reinforcing steel resist the shear forces along the cracks. It has already been pointed out that the dowel forces offer approximately one third the resistance of the aggregate particle interlocking forces. Consequently for the wide cracks there is a tendency to distort the reinforcing steel crossing the crack. This was evident in panel B where the shear forces produced a 'Kink' in the reinforcing bars and the high local stress caused some crushing of the concrete.

7.1.3 Comparison of Stiffness Deterioration

A comparison of the stiffness degradation of the four wall panels is presented in Figure 38. The stiffness at a given cycle was calculated considering only the initial slope of the load-deflection curves. For cases where a steepening of the curves occurred due to the closing of cracks, an average value of the two slopes was considered to represent the stiffness of that cycle. No modifications were made if cracking caused the load-deflection curve to flatten out.

The stiffness values of the four panels, as presented in Figure 38 shows that in many cases there was a large reduction in stiffness during the second cycle of the series of three cycles at the same displacement. In the initial cycle further cracking occurred and the effect on the initial stiffness is not observed until the following cycle. This phenomena is more evident in the stiffness values of panels C and D where cracking occurred throughout the thirteen cycles of lateral loading. While there is a reduction in stiffness deterioration between the second and third cycles of the series at the same displacement, insufficient cycles were undertaken to determine whether a stabilization of the stiff-

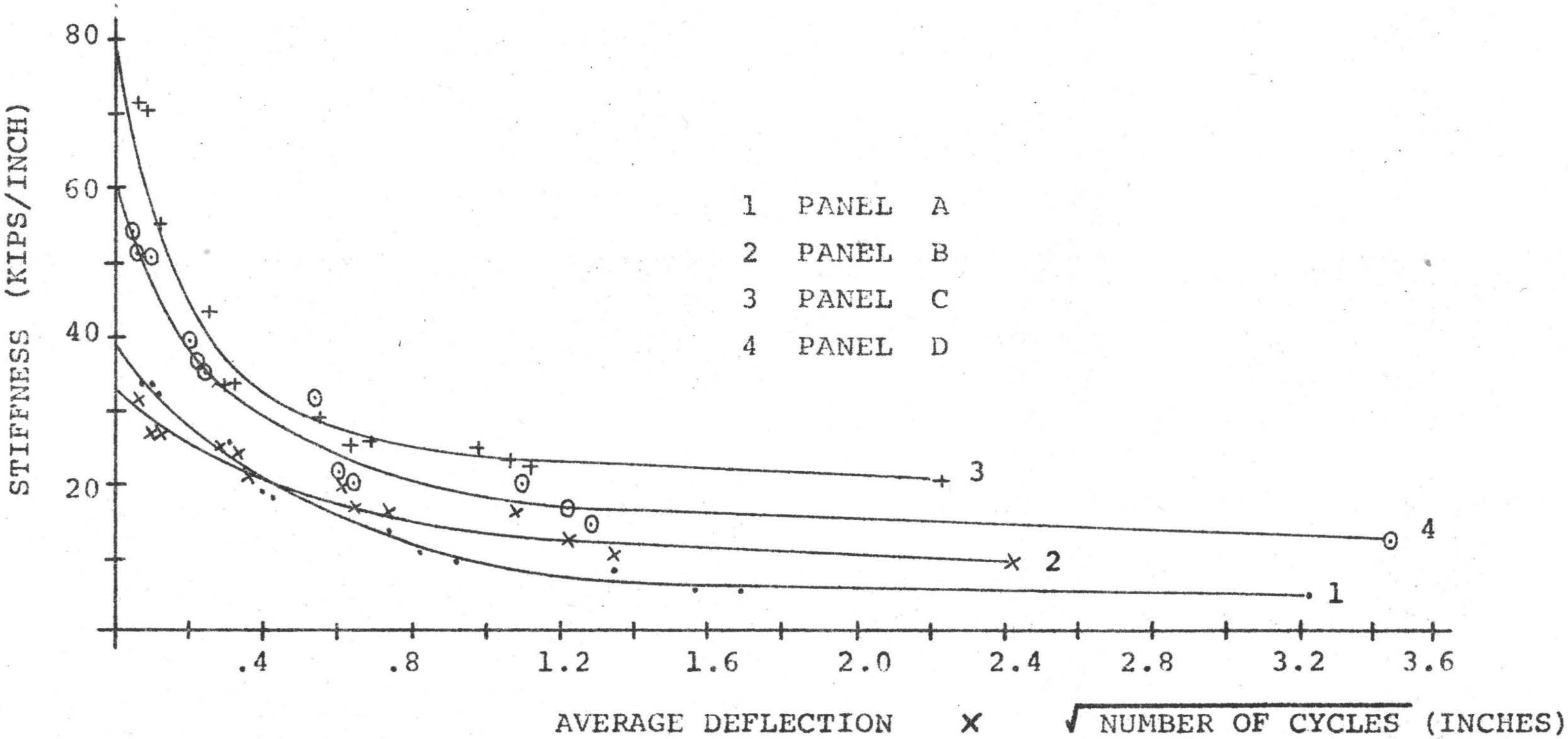

FIG. 38 STIFFNESS DEGRADATION OF WALL PANELS

ness deterioration occurs.

7.1.3.1 Effect of Vertical Slits

Figure 38 indicates that the initial stiffness of panel A, the slitted wall, and panel B, the ordinary reinforced concrete wall was essentially the same. In the elastic range of these two walls the lateral displacements were small and errors in the recorded values would greatly influence the calculated stiffness.

After the formation of the initial cracks the stiffness behaviour of the two walls differed. Figure 39 and 40 show that the stiffness deterioration of the slitted wall panel was more rapid than that of the ordinary reinforced concrete wall and that the final value of stiffness was lower. The difference between the two walls is due to the different cracking behaviour.

The initial cracks in panels A and B were due to flexural stress and formed at each end between the lower flange beam and the wall section. The subsequent cracking patterns in the two wall panels differed considerably. Diagonal cracks formed in the slitted wall panel between the ends of the slits and the flange beams. The vertical slits acted as lines of weakness and induced a particular pattern on the wall panel. In contrast, further cracking in the reinforced concrete wall was restricted to a few diagonal cracks at each end and additional cracking along the flange beam-wall interface.

The stiffness deterioration was more rapid and the

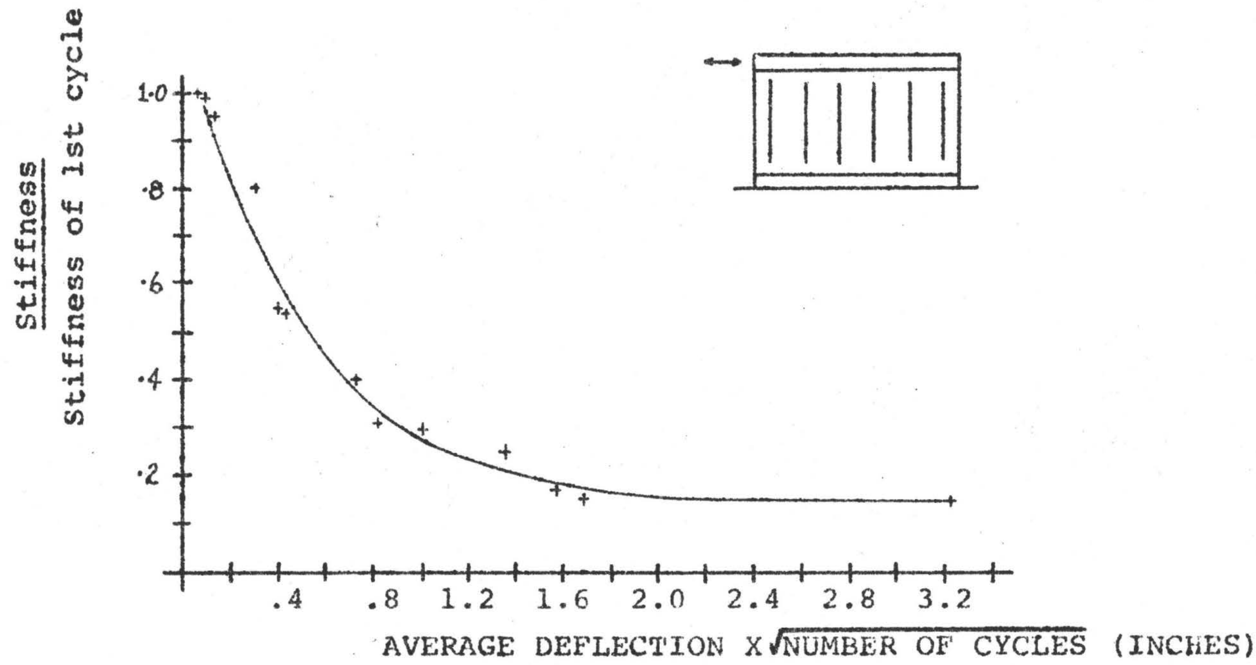

Fig. 39 STIFFNESS DEGRADATION OF PANEL A

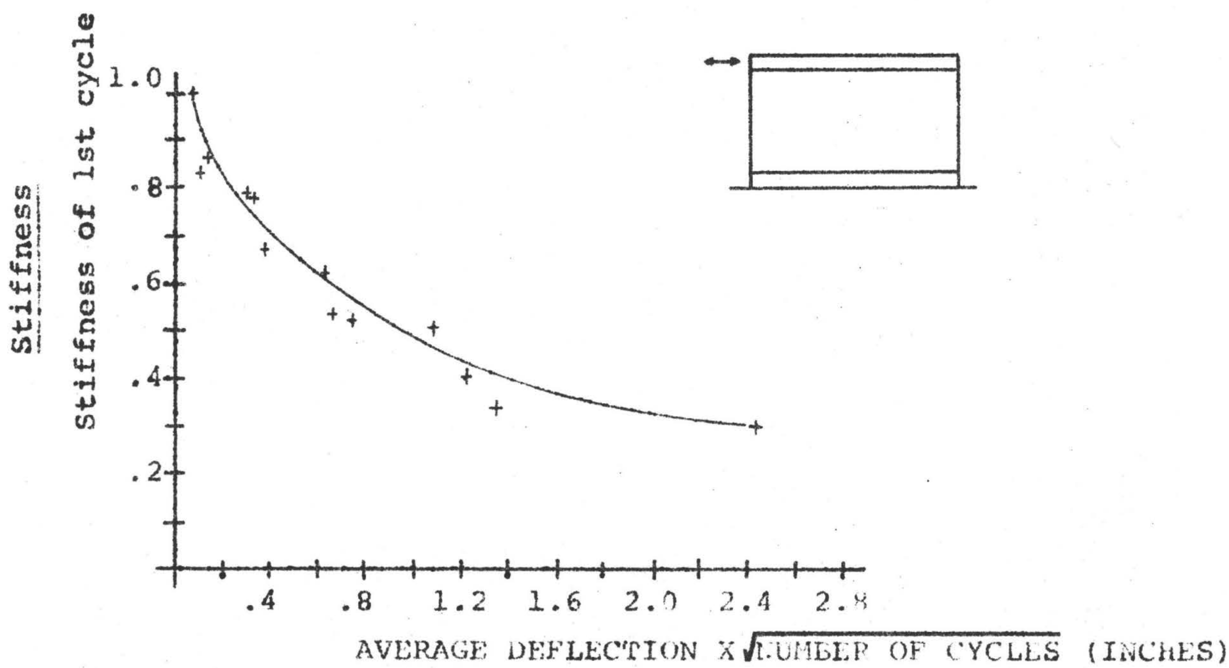

Fig. 40 STIFFNESS DEGRADATION OF PANEL B

final stiffness value smaller in the slitted wall as little resistance to cracking was offered by the vertical slits. Relative movement along the slits was not restricted by transverse reinforcing or by the uneven surface of a normal crack. Consequently the crack pattern of panel A offered less resistance to lateral load.

7.1.3.2 Effect of Vertical Loads

An increase in stiffness of the two wall panels under vertical load is displayed in Figure 38. A study of the effects of axial loads on a reinforced concrete beam subjected to repeated loading has shown that the hysteresis loops are strongly influenced by the axial loads[41]. The increase in the initial stiffness of the shear walls subjected to vertical and lateral loads can be explained by likening this situation to a concrete compression cylinder laterally restrained by fluid pressure. The lateral restraining pressure causes an increase in strength and stiffness of the concrete cylinder[24]. A similar increase will occur in the wall panels.

The initial rate of stiffness deterioration after first cracking seems to be unaffected by the presence of vertical load. The rates of stiffness deterioration of the two standard slitted panels are shown in Figures 39 and 41. The final stiffness value of panel A is less than the final value of panel C due to the formation of the larger crack widths.

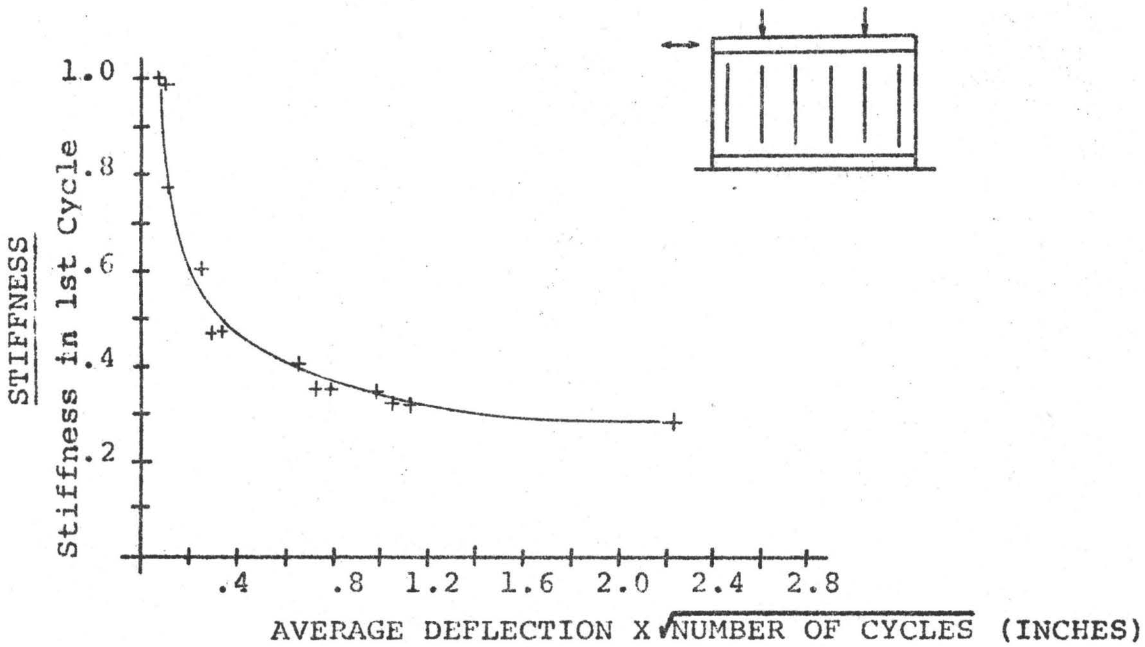

Fig. 41 STIFFNESS DEGRADATION OF PANEL C

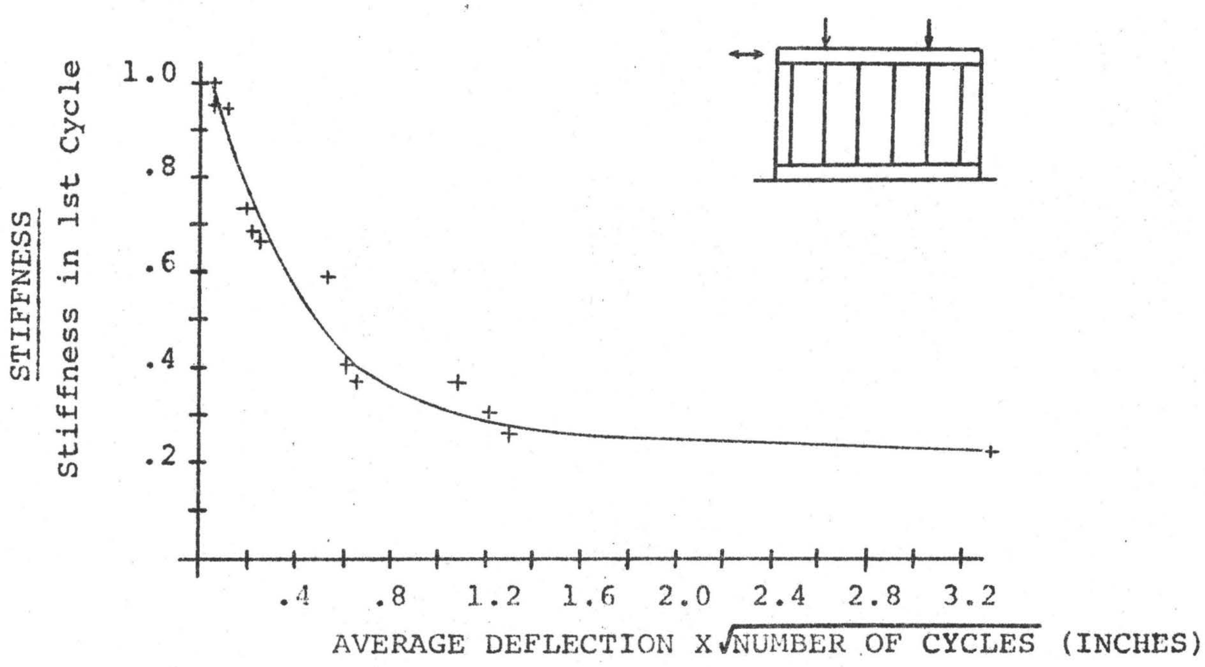

Fig. 42 STIFFNESS DEGRADATION OF PANEL D

7.1.3.3 The Effect of Lengthening the Vertical Slits to Full Panel Height

A comparison of the stiffness results of panels C and D (Figure 41 and 42) shows the effect of lengthening the slits to the full panel height. A decrease is shown to occur both in the rate of deterioration and in the initial and final stiffness values. The difference in the initial stiffness is probably due to the inclusion of the panel high vertical slits which, because the asbestos is less rigid than the concrete, enabled the wall to undergo greater deformations without cracking. The panel high vertical slits altered the final crack pattern and consequently influenced the resistance mechanism for lateral loading. A relatively flexible mechanism was developed in panel D by the extensive cracking along the lower flange beam-wall interface and by the relative movement along the vertical slits. The mechanism of panel C was stiffer and it involved the vertical slits, the diagonal cracks between the ends of the slits and the flange beams and the flexural cracks in the flange beam-wall interfaces. Hence the final stiffness value is greater for panel C.

7.2 Energy

7.2.1 Introduction

The response of a structure to seismic ground motions can be assessed by considering the energy properties of the structural components. The considerations must involve both the ability of the component to absorb and to dissipate energy. The absorption of energy depends on the load required to produce yielding and on the amount of inelastic deformations a component can undergo before failure. If the inelastic deformation after yielding is small the inelastic strength reserve is low and failure of the component may result.

7.2.2 Ductility Factors

The ductility factor, the ratio of total displacement to the yield displacement, is a useful parameter for the comparison of energy absorption. The ductility factors of the four wall panels are displayed in Table 2. According to current earthquake engineering design practice a ductility factor of 5.1 for an ordinary reinforced concrete wall indicates a satisfactory component. Two further points should be noted about these ductility values.

In the first place the walls were not laterally loaded to the point of failure due to a deformation limitation imposed by the loading frame. The failure point of the wall is considered to be reached when the lateral load significantly decreases with further lateral displacements. The load-deflection diagrams of Figure 32, 33, 34, and 35 indicate that the failure point was not reached in any of the four tests. A slight modification of the loading frame will enable future panels to be tested to failure.

Secondly the determination of ductility factors for

PANEL TYPE	DUCTILITY FACTORS
PANEL A	6.2
PANEL B	5.1
PANEL C	16.0
PANEL D	18.3

TABLE 2 DUCTILITY FACTORS

reinforced concrete members is a difficult process. In many cases the yield point or the position where the component starts to behave inelastically is not well defined. This is the case in panel A where a change in slope occurred between the first and fourth cycles of lateral loading. This change of slope occurred before the formation of the first visible cracks. For panel A the displacement at first cracking was used to determine the ductility factor.

7.2.3 Energy Dissipation

The ability of the structural components to dissipate energy indicates how the structure will respond to the earthquake ground motions. If the energy dissipation is large the vibrational response of the structure will be small. Conversely if the energy dissipation is small a build up of the absorbed energy will create a violent vibrational response which may lead to failure of the structural components if the total inelastic displacement capacity is exceeded.

A comparison of the amounts of energy dissipated by each panel is presented in Figure 43. The energy dissipation values were calculated by determinnng the area within each hysteresis loop. Three observations can be made from this diagram.

1. The ordinary reinforced concrete wall (panel B) dissipates more energy than the slitted wall (panel A).
2. An increase in the amount of energy dissipated occurs when the panels are subjected to vertical loads.

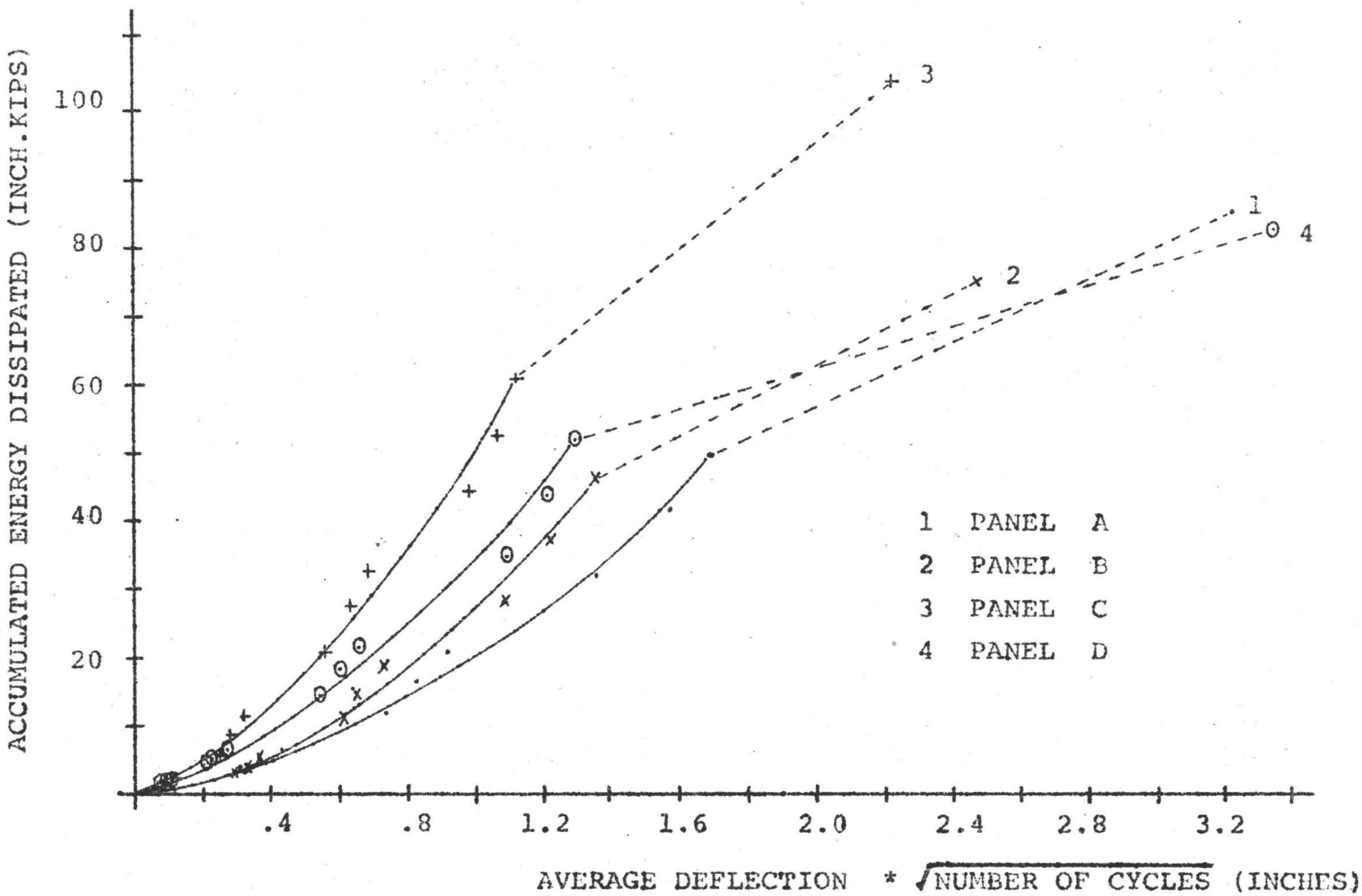

Fig. 43 ENERGY DISSIPATED BY THE WALL PANELS

3. A reduction in the amount of energy dissipated results from the lengthening of the vertical slits to the full height of the wall panel.

7.2.4 Energy Dissipating Processes

An explanation for the above observations can be found in the energy dissipating processes. In this investigation three processes were identified but due to the limited number of wall panels tested only a general discussion can be given.

7.2.4.1 Cracking

The primary energy dissipating processes appears to be the formation of cracks. Figure 43 shows that before cracking very little energy was dissipated and it is only in the fourth cycle, after the initial cracks have occurred, that significant amounts of energy are dissipated. In panels C and D, which display better energy dissipating properties, the formation of the cracks was spread throughout the remaining lateral loading cycles. The cracking in panel C was extensive while a large portion of the cracks in panel D formed in the lower flange beam. In comparison, the formation of cracks in panels A and B essentially ceased after the seventh cycle. Consequently both the length of cracks and the thickness of the cracked section appear to be important factors in this mode of energy dissipation.

The process of crack formation has been investigated at some length[31] but no attempt has been made to define the variables of energy dissipation during cracking. Energy methods, however, have been used to explain the formation of cracks[42]. The theory of fracture strength suggested by Griffith for a brittle material has been modified to take into account the dissipation of strain energy in plastic flow. A detailed study of the entire process of energy dissipation during cracking may add considerably to the knowledge of the inelastic behaviour of reinforced concrete members.

Even though cracking in panels A and B had essentially ceased after the seventh cycle, Figure 43 shows that the amount of energy dissipated increased with further inelastic displacement. Two energy dissipating processes were identified which can account for this increase.

7.2.4.2 Crack Widening

The first process was the widening of cracks. This was most noticeable in the region of the flexural cracks in panels A and B and the process involved a breakdown of the bond forces and an extension of the reinforcing steel crossing the crack. Additional energy was dissipated when the lateral load was reversed and the cracks closed.

7.2.4.3 Slippage and Relative Movement Along the Cracks

The second process was slippage and relative movement along the cracks. Energy was dissipated in this process by overcoming the frictional forces existing between the aggregate particles in the surfaces of the cracks and by producing inelastic deformations of the reinforcing steel.

The relative amounts of energy dissipated by the three cycles at the same lateral displacements supports the premise that crack formation is the major energy dissipating process. In the first cycle, during which most of the cracking occurred, more energy was dissipated. The dissipation of energy in the remaining two cycles was limited to the widening of cracks and to relative movement along the cracks.

7.2.5 Comparison of Energy Dissipation

7.2.5.1 The Effect of Vertical Slits

The ordinary reinforced concrete wall dissipated more energy than the slitted wall panel. The difference was due to the formation of different crack patterns. The final crack pattern of panel A, as previously discussed, was considerably influenced by the inclusion of the vertical slits. The resistance mechanism involved relative movements along the vertical slits. Little energy was dissipated in the breakdown of the adhesive forces between the concrete and the asbestos sheets and the relative movement along the slits was not restricted by transverse reinforcing or by the uneven surfaces that occur in a normal crack. Consequently the inclusion of vertical slits in the wall panels reduces the ability to dissipate energy.

7.2.5.2 The Effect of Vertical Loads

More energy was dissipated by the standard slitted panel which was subjected to both horizontal and vertical loads. As has been explained previously the cracking process of energy dissipation accounted for this large increase.

7.2.5.3 The Effect of Lengthening the Slits to the Full Panel Height

The lengthening of the vertical slits to the full height of the wall panel resulted in a decrease in the amount of energy dissipated. The inclusion of the panel high vertical slits produced a different pattern of cracks. The cracking in panel D was not nearly as extensive as panel C and hence the energy dissipated by the process of cracking was reduced. As little relative movement occurred along the cracks and the width of the cracks remained small in panel D the total energy dissipated was less than that of panel C.

CHAPTER VIII

CONCLUSIONS AND RECOMMENDATIONS

8.1 Conclusions

A comparison of the different behaviours of the four wall panels of this investigation indicates that the inclusion of vertical slits does not improve the performance of reinforced concrete wall panels under repeated cycling lateral loading. The application of vertical loads was shown to have a beneficial effect while the lengthening of the vertical slits to the full panel height was shown to be detremental to the overall performance of the wall panel. The system of applying the vertical loads influenced the pattern of cracks but it is not known to what extent the various properties were affected by this loading process.

8.1.1 Energy Properties

All four wall panels displayed sufficient inelastic deformations and energy absorption capabilities for most practical cases. The inclusion of vertical slits in reinforced concrete panels reduced the amount of energy dissipated while an increase in energy dissipation was experienced from the application of vertical loads. A decrease in energy dissipation also occurred when the vertical slits were lengthened to the full panel height.

8.1.2 Stiffness Deterioration

A large deterioration of stiffness occurred in all walls. The vertical slits increased the rate of deterioration and lowered the final stiffness values. The application of vertical loads did not affect the initial rate of deterioration but it did raise the initial and final stiffness values. The rate of stiffness deterioration was reduced and the initial and final value of stiffness decreased by the lengthening of the vertical slits to the full panel height.

8.1.3 Cracking

The pattern of crack formation was influenced by both the vertical slits and by the application of the vertical loads. The vertical slits acted as lines of weakness and thereby induced diagonal cracks between the ends of the slits and the flange beams. The presence of vertical loads suppress the formation of the flexural cracks and induced mainly diagonal cracking.

8.1.4 Load Carrying Characteristics

The inclusion of vertical slits caused a reduction in the load carrying capacity of reinforced concrete wall panels while an increase was experienced when the panels were subjected to vertical loads. The load carrying capacity decreased on lengthening the vertical slits to the full height of the panel.

8.2 Suggestions for Further Research

8.2.1 The experimental investigation showed that a reinforced concrete wall panel with a length to height ratio of two and a reinforcing ratio of 0.25 per cent behaved satisfactorily under repeated cyclic lateral loads. Further tests should be undertaken on reinforced concrete walls to determine the effects of reinforcing ratio, reinforcing arrangement and length to height ratio on the stiffness deterioration and on the energy properties.

8.2.2 Vertical loads were shown to influence the lateral response of the wall panels. More research is required to fully investigate the effect of both tensile and compressive axial forces on the lateral response of wall panels.

8.2.3 A detailed investigation into the various energy dissipating mechanics involved in the process of cracking in reinforced concrete members may add considerably to the knowledge of the inelastic behaviour of reinforced concrete.

REFERENCES

1. Beckmann P. and Duncan P.: "The Use of Shear Walls in High Buildings", Proceedings of a Symposium on Tall Buildings, University of Southampton, April 1966.

2. Frischmann W.W. and Prabher S.S.: "Planning Concepts of Shear Walls", Proceedings of a Symposium on Tall Buildings, University of Southhampton, April 1966.

3. Khan Fazlur R.: "Current Trends in Concrete High Rise Buildings", Proceeding of a Symposium on Tall Buildings, University of Southhampton, April 1966.

4. Beck H.: "Contribution to the Analysis of Coupled Shear Walls", Proceeding of ACI Journal, Vol. 59, No. 8, August 1962.

5. Rosman R.: "Approximate Analysis of Shear Walls Subjected to Lateral Loads", Proceeding of ACI Journal, Vol. 61, No. 6, June 1964.

6. Coull A. and Choudhury J.R.: "Analysis of Coupled Shear Walls", Proceeding of ACI Journal, Vol. 64, No. 9, September 1967.

7. Coull A. and Stafford Smith B.: "Analysis of Shear Wall Structures, (A review of Previous Research)", Proceeding of a Symposium on Tall Buildings, University of Southhampton, April 1966.

8. Stafford Smith B.: "Modified Beam Method for Analysing Symmetrical Interconnected Shear Walls", Proceeding of ACI Journal Vol. 67, No. 12, December 1970.

9. Macleod T.A.: "Lateral Stiffness of Shear Walls With Openings", Proceedings of a Symposium on Tall Buildings, University of Southhampton, April 1966.

10. National Research Council of Canada, "National Building Code of Canada 1970", Publication N.R.C. No. 11246 Ottawa, Canada, 1970.

11. Structural Engineers Association of California, "Recommended Lateral Force Requirements", 1966.

12. Steinbrugge Karl V., Manning John H. and Degenkolb Henry J.: "The Prince William Sound, Alaska, Earthquake of 1964 and aftèr shocks", U.S. Dept. of Commerce. Environmental Science Service Administration.

13. Steinbrugge Karl V.: "Earthquake Damage and Structural Performance in the United States". Chapter 9 in Earthquake Engineering, edited by Robert L. Wiegel, Prentice-Hall, Inc. 1970, pp. 167-226.

14. Winokur A. and Gluck J.: "Ultimate Strength Analysis of Coupled Shear Walls", Proceedings of ACI Journal, Vol. 65, No. 12, December 1968.

15. Paulay T.: "An Elasto-Plastic Analysis of Coupled Shear Walls", Proceedings of ACI Journal, Vol. 67, No. 11, November 1970.

16. Benjamin J.A. and Williams H.A.: "The Behaviour of One-Story Reinforced Concrete Shear Walls", Proceeding, Structural Division ASCE, Vol. 83, No. ST3, May 1957.

17. Benjamin J.A. and Williams H.A.: "The Behaviour of One-Story Reinforced Concrete Shear Walls Containing Openings". Proceedings ACI Journal, Vol. 55, No. 5, November 1958.

18. Muto Kiyoshi: "Earthquake Resistant Design of 36-Storied Kasumigaseki Building" Proceeding, Fourth World Conference on Earthquake Engineering, 1969 Chile.

19. Muto Kiyoshi: "Newly-Devised Reinforced Concrete Shear Walls for High Rise Building Structures" SEAOC Convention of Hawaii, October 1969.

20. Muto Kiyoshi: "Earthquake Proof Design Gives Rise to First Japanese Skyscrapers", Proceeding of Civil Engineering, ASCE, Vol. 41, No. 3, March 1971.

21. Paulay T.: "Coupling Beams of Reinforced Concrete Shear Walls". Proceedings Structural Division ASCE, Vol. 97, No. ST3, March 1971.

22. Paulay T., "The Coupling of Shear Walls", thesis presented for the degree of Doctor of Philosophy in Civil Engineering at the University of Canterbury Christchurch, New Zealand.

23. American Concrete Institute, "Building Requirements for Reinforced Concrete - Proposed Revisions of ACI 318-63", Proceeding of ACI Journal Vol. 67, No. 2, February 1970.

24. Blume J.A., Newmark N.M. and Corning L.A.: "The Design of Multistory Reinforced Concrete Buildings for Earthquake Motions". Portland Cement Association 1961.

25. Singh Awtar, Gerstle Kurt H., and Tuli Leonard G.: "The Behaviour of Reinforcing Steel Under Reverse Loading" Proceeding of Material Research and Standards, January 1965, Vol. 5, No. 1.

26. Johnston R.P. "Structural Concrete", McGraw-Hill Publishing Company Limited, 1967.

27. Paulay T.: "Reinforced Concrete Shear Walls", New Zealand Engineer, 15th October 1969.

28. Stafford Smith Bryan: "Model Test Results of Vertical and Horizontal Loading of Infilled Frames", Proceeding ACI Journal, Vol. 65, No. 8, August 1968.

29. Hansen Norman W. and Connor Harold W.: "Seismic Resistance of Reinforced Concrete Beam-Column Joints", Proceeding Structural Division ASCE, Vol. 93, No. ST5 October 1967.

30. Popov Egor P. and Pinkney P. Bruce: "Cyclic Yield Reversal in Steel Building Connections", Proceeding Structural Divisions ASCE, Vol. 95, No. ST3, March 1969.

31. Shah Surendra P. and Winter George: "Inelastic Behaviour and Fracture of Concrete", Causes, Mechanism, and Control of Cracking in Concrete. Special publication, ACI SP.20.

32. Kani G.N.J.: "The Riddle of Shear Failure and its Solution", Proceeding of ACI Journal, Vol. 61, No. 4, April 1964.

33. Fenwick R.C. and Paulay T.: "Mechanism of Shear Resistance of Concrete Beams", Proceeding Structural Division ASCE, Vol. 94 No. ST10, October 1968.

34. Timoshenko S. and Young D.H.: "Elements of Strength of Materials", D. Van Nostrand Company INC. 1968.

35. Medearis Kenneth and Young D.H.: "Energy Absorption of Structures under Cyclic Loading", Proceedings Structural Division ASCE, Vol. 90, No. ST1, February 1964.

36. Blackely R.N.G., Park R. and Shepherd R.: "A Review of Seismic Resistance of Prestressed Concrete" Bulletin New Zealand Society of Earthquake Engineers.

37. Jacobsen Lydik S.: "Damping in Composite Structures", Proceeding of the Second World Conference of Earthquake Engineering, Japan 1960.

38. Bresler Boris and Berlero Vilelomo: "Behaviour of Reinforced Concrete under Repeated Loads" Proceedings Structural Division ASCE, Vol. 94, No. ST6, June 1968.

39. Agrawal G.L., Tulen Leonard G. and Gerstle Kurt H.: "Response of Doubly Reinforced Concrete Beams to Cyclic Loading" Proceeding of ACI Journal, Vol. 62, No. 7, July 1965.

40. Lutz Leory A. and Gergely Peter: "Mechanics of Bond and Slip of Deformed Bars In Concrete", Proceedings of ACI Journal, Vol. 64, No. 11, November 1967.

41. Yamada Minora: "Low cycle fatique fracture limits of various Kinds of Structural Members Subjected to Alternately repeated Plastic Bending under Axial Compression as an Evaluation Basis or Design Criteria for Seismic Capacity", Proceeding of the Fourth World Conference on Earthquake Engineering, Chile 1969.

42. Kaplan M.F.: "Crack Propagation and the Fracture of Concrete", Proceeding of ACI, Vol. 58, No. 5, Nov. 61.